

Wave-wave interactions in finite depth water

Ray Q. Lin

Hydromechanic Directorate, David Taylor Model Basin, Carderock Division, West Bethesda, Maryland

Will Perrie

Physical and Chemical Science, Department of Fisheries and Oceans, Bedford Institute of Oceanography
Dartmouth, Nova Scotia, Canada

Abstract. In this study we present a new formulation for the nonlinear wave-wave interaction source function in finite water depth. The formulation, denoted the reduced integration approximation (RIA), is shown to compare well with published formulations, both for shallow water wave-wave interactions [Herterich and Hasselmann, 1980; Polnikov, 1997; Hashimoto *et al.*, 1998; A. Masuda and K. Komatsu, manuscript in preparation, 1998] and also for the asymptotic deep water limit: (1) the Hamiltonian formulation proposed by Lin and Perrie [1997], by (2) Hasselmann and Hasselmann [1981], and (3) the line integral transformation of Webb [1978] and Resio and Perrie [1991]. Of these deep water formulations, that of Lin-Perrie generalizing the Hamiltonian representation of Zakharov [1968] to finite depth water, is notable for its simplicity, efficiency and its ability to apply to very shallow water ($kh \approx 0.3$), and highly nonlinear ($\varepsilon \leq 0.3$) interactions. RIA is based on an analysis of the main resonance domain, which reduces the six-dimensional integration to a quasi-line integral to minimize computational time. In terms of computational time, RIA is a thousand times faster than the EXACT-NL version formulated by Hasselmann and Hasselmann [1981], with similar accuracy. Thus RIA can be considered a candidate for operational forecasting in finite depth water, in the sense that the discrete interaction approximation was presented as a candidate for operational deep water wave forecasting by Hasselmann *et al.* [1988].

1. Introduction

The importance of the nonlinear source term in a wave model needs no emphasis. In an operational wave forecast model, 25–50% of the computation time is used for evaluating the nonlinear source function. Recently, Young and Van Vledder [1993] and Komen *et al.* [1994] have given a comprehensive review of the history of past efforts to evaluate this term effectively. The state of the art, in operational wave models, is still the discrete integration approximation (DIA) method proposed by Hasselmann and Hasselmann [1985] for operational models, and the EXACT-NL formulation of Hasselmann and Hasselmann [1981] for research models. By introducing DIA, Hasselmann *et al.* [1988] provided the possibility of having a fully discrete spectral wave model that is based on solving the energy balance equation, which was not possible before this time. In particular, DIA made possible the introduction of explicit source functions for input and dissipation. With some tuning, DIA and Wave Model (WAM) are able to produce reasonable deep water growth curves. Scaling allowed some accommodation for finite depth conditions. Therefore DIA represents a genuine milestone in the development of operational wave modeling.

However, it is impossible for a parameterization such as DIA to satisfy all possible different spectral wave shapes, especially because the nonlinear transfer is very sensitive to both the shape of spectrum and the water depth. Sensitivity of the nonlinear transfer to angular resolution follows because the

distribution of the resonant solutions is highly nonlinear, as reported by Phillips [1960] and Fox [1976]. Moreover, for extremely shallow water, quasi-resonant three-wave interactions will transfer energy within the spectrum, as discussed by Eldeberky [1996], although they do not theoretical satisfy the resonance conditions for energy transfer. Therefore any apparent ability of widely differing operational models (first, second, and third generation) to predict the sea state with equal success, as suggested by Cardone *et al.* [1995], reflects both model tuning, as well as test storms which do not produce conditions that deviated sufficiently from classical empirical growth curves, to which the models were tuned.

Although DIA is very practical and EXACT-NL is very elegant, the former has not been shown to work well for shallow water, and the latter is not efficient enough for operational work. The motivation of this study is to find an accurate and efficient method to evaluate the nonlinear wave-wave interactions for finite depth water in the coastal region. The origin of the nonlinear source function can be traced to the pioneering studies by Hasselmann [1962], who applied perturbation theory to fifth-order and obtained the energy transfer rate between four-wave components for finite depth water. This result has been recognized as a standard formulation for more than 3 decades. More recently, this work was extended by Herterich and Hasselmann [1980], Hashimoto *et al.* [1998], A. Masuda and K. Komatsu (manuscript in preparation, 1998), and to finite depth water. However, the Hasselmann [1962] formulation is not only limited to weak nonlinear interactions ($\varepsilon \leq 0.06$) but also to water that is not too shallow ($kh \geq 0.7$), as suggested by Herterich and Hasselmann [1980]. Furthermore, it is too complicated to be of any practical use in describing the

Copyright 1999 by the American Geophysical Union.

Paper number 1999JC900026.
0148-0227/99/1999JC900026\$09.00

sea state evolution, especially in an operational wave forecast model. *Longuet-Higgins* [1976] and *Fox* [1976] used a simplified approach to estimate the nonlinear wave-wave interaction energy transfer for deep water. However, they concentrated on the interaction of the components near the spectral peak, using a limited number of degrees of freedom. Although effective, this approach cannot be used for a discretized spectrum, which is used by WAM. Moreover, this method is not in good agreement with the results obtained through a more exact integration by *Hasselmann and Hasselmann* [1981]. The discrepancies are especially pronounced in the determination of the locations of minimum and zero values.

A breakthrough in evaluating the nonlinear source function S_{nl} was proposed by *Webb* [1978] and *Masada* [1980], who derived a equivalent but much simpler deep water formulation, compared to that of *Hasselmann* [1962]. This simplified formulation led to a new integration method for S_{nl} , in addition to EXACT-NL, the classical integration method for S_{nl} . This new method was implemented in the similarity scaling method (SSM) formulation of *Tracy and Resio* [1982] and *Resio and Perrie* [1991] in studies of the nonlinear source function in deep water. The SSM formulation, which uses scaling and phase space terms to replace the full integration variables with transformed variables, generated an opportunity to accurately calculate the nonlinear energy transform. This was verified by comparisons with the classical investigations of *Hasselmann and Hasselmann* [1981], as reported by *Resio and Perrie* [1991]. However, the speed of SSM is still much too slow to be used in the operational model. Yet for research purposes, it has proven to be of value, as shown by *Young and Van Vledder* [1993].

Recently, *Snyder et al.* [1993] proposed a hybrid scheme for the *Hasselmann* [1962] formulation to simulate the nonlinear action transfer rate. However, this method is only ~ 20 times faster than the original full integration given by *Hasselmann and Hasselmann* [1985], for the spectral frequency-direction resolution of our integrations. Moreover, because the hybrid method has to invoke the assumption that the spectral function is piecewise constant basis and pre-sums coefficients, it divides the frequency domain into 16 bins and the angle domain into 10 bins. For such low resolution, the solutions by *Snyder et al.* [1993] may be similar to EXACT-NL. However, for high resolution, the solutions by *Snyder et al.* [1993] will significantly differ from EXACT-NL. This is because the piecewise constant assumption distributes the resonant solutions linearly. However, the resonant solutions are highly nonuniformly distributed in the real world [*Phillips*, 1960; *Fox*, 1976].

As discussed by *Lin and Perrie* [1997, hereafter referred to as LP97], *Zakharov's* method is more elegant and has a much simpler algebraic formulation than *Hasselmann's* formulation, which leads to a greater efficiency in the initialization of the computation and also to greater accuracy in strongly nonlinear situations [*Crawford et al.*, 1981]. The former is based on a Hamiltonian formulation whereas the latter is based on a Boltzmann integral derived from perturbation expansions. *Herterich and Hasselmann* [1980] suggest that the Boltzmann integral method will break down when $kh \leq 0.7$, whereas the Hamiltonian formulation remains valid until $kh \leq 0.3$. LP97 extended *Zakharov's* calculation and obtained a new formulation for the nonlinear energy transfer due to wave-wave interactions in finite depth water with nonlinear dispersion. LP97 also found that wide band instability dominates in shallow water, instead of narrowband instability. Moreover, *Zakharov* [1998] pointed out that the nonlinear transfer rate in shallow

water is extremely sensitive to water depth, shape of the spectrum, and spreading angle.

In this paper, we are concerned with obtaining an accurate and efficient formulation for the nonlinear wave-wave interactions suitable for operational wave forecasting in finite depth water. The theoretical basis for our presentation is found in LP97. In the following sections, we present our reduced interaction approximation (RIA), and we compare our simulations with the finite depth simulations of *Herterich and Hasselmann* [1980], *Polnikov* [1997], *Hashimoto et al.* [1998], and A. Masuda and K. Komatsu (manuscript in preparation, 1998) as well as the asymptotic deep water simulations of LP97, *Resio and Perrie* [1991] and *Hasselmann and Hasselmann* [1981]. In order to make these comparisons, we use linear dispersion in the following computations, which assumes $\omega^2 = gk \tanh kh$. Nonlinear dispersion, which will be presented in a related paper, generally leads to smaller nonlinear transfers, especially in shallow water.

2. Reduced Integration Approximation

In the following paragraphs, we are going to introduce a new integration method, which achieves a reduction of the integration dimensions in order to speed up the integration. We will show that the full six-dimensional integration can be reduced to a quasi-line integration, which we denote as RIA.

From LP97, we know that the nonlinear action transfer rate for wave-wave interactions in finite depth water is given by

$$\begin{aligned} \frac{\partial A_{(k_i)}}{\partial \tau} = & 4\pi \int \int \int_{-\infty}^{\infty} T_{i,1,2,3}^2 \delta(\mathbf{k}_i + \mathbf{k}_1 - \mathbf{k}_2 - \mathbf{k}_3) \\ & \cdot \delta[\omega_{(k_i)} + \omega_{(k_1)} - \omega_{(k_2)} - \omega_{(k_3)}] \\ & \cdot \{A_{(k_1)} A_{(k_2)} [A_{(k_1)} + A_{(k_2)}] \\ & - A_{(k_1)} A_{(k_3)} [A_{(k_3)} + A_{(k_2)}]\} d\mathbf{k}_1 d\mathbf{k}_2 d\mathbf{k}_3, \end{aligned} \quad (1a)$$

where

$$\begin{aligned} T_{i,1,2,3} = & -V_{(k_3, k_3-k_1, k_1)}^{(-)} V_{(k_i, k_2, k_i-k_2)}^{(-)} \\ & \cdot \left\{ \frac{1}{\omega_{(k_1-k_3)} - \omega_{(k_3)} + \omega_{(k_1)}} + \frac{1}{\omega_{(k_2)} + \omega_{(k_i-k_2)} - \omega_{(k_i)}} \right\} \\ & - V_{(k_2, k_i, k_2-k_i)}^{(-)} V_{(k_1, k_1-k_3, k_3)}^{(-)} \\ & \cdot \left\{ \frac{1}{\omega_{(k_1-k_3)} - \omega_{(k_1)} + \omega_{(k_3)}} + \frac{1}{\omega_{(k_i)} + \omega_{(k_3-k_i)} - \omega_{(k_2)}} \right\} \\ & - V_{(k_2, k_2-k_1, k_1)}^{(-)} V_{(k_i, k_3, k_i-k_3)}^{(-)} \\ & \cdot \left\{ \frac{1}{\omega_{(k_1-k_2)} - \omega_{(k_2)} + \omega_{(k_1)}} + \frac{1}{\omega_{(k_3)} + \omega_{(k_3-k_i)} - \omega_{(k_i)}} \right\} \\ & - V_{(k_3, k_i, k_3-k_i)}^{(-)} V_{(k_1, k_1-k_2, k_2)}^{(-)} \\ & \cdot \left\{ \frac{1}{\omega_{(k_1-k_2)} - \omega_{(k_1)} + \omega_{(k_2)}} + \frac{1}{\omega_{(k_i)} + \omega_{(k_3-k_i)} - \omega_{(k_3)}} \right\} \\ & - V_{(k_i+k_1, k_i, k_1)}^{(-)} V_{(k_2+k_3, k_2, k_3)}^{(-)} \\ & \cdot \left\{ \frac{1}{\omega_{(k_i+k_1)} - \omega_{(k_i)} - \omega_{(k_1)}} + \frac{1}{\omega_{(k_2+k_3)} - \omega_{(k_2)} - \omega_{(k_3)}} \right\} \\ & - V_{(-k_2-k_3, k_2, k_3)}^{(+)} V_{(k_i, k_1, -k_i-k_1)}^{(+)} \end{aligned}$$

$$\cdot \left\{ \frac{1}{\omega_{(\mathbf{k}_2+\mathbf{k}_3)} + \omega_{(\mathbf{k}_2)} + \omega_{(\mathbf{k}_3)}} + \frac{1}{\omega_{(\mathbf{k}_i+\mathbf{k}_1)} + \omega_{(\mathbf{k}_i)} + \omega_{(\mathbf{k}_1)}} \right\} + \bar{W}_{(\mathbf{k}_i, \mathbf{k}_1, \mathbf{k}_2, \mathbf{k}_3)}, \quad (1b)$$

in which

$$V_{(\mathbf{k}_i, \mathbf{k}_1, \mathbf{k}_2)}^{(\pm)} = \frac{1}{8\pi\sqrt{2}} \left\{ [\mathbf{k}_i \cdot \mathbf{k}_1 \pm k_i k_1 \tanh(k_i)h \tanh(k_1)h] \cdot \left[\frac{\omega_{(k_i)}\omega_{(k_1)}k_2 \tanh k_2 h}{\omega_{(k_2)}k_i k_1 \tanh k_i h \tanh k_1 h} \right]^{1/2} + [\mathbf{k}_i \cdot \mathbf{k}_2 \pm k_i k_2 \tanh(k_i)h \tanh(k_2)h] \cdot \left[\frac{\omega_{(k_i)}\omega_{(k_2)}k_1 \tanh k_1 h}{\omega_{(k_1)}k_i k_2 \tanh k_i h \tanh k_2 h} \right]^{1/2} + [\mathbf{k}_1 \cdot \mathbf{k}_2 + k_1 k_2 \tanh(k_1)h \tanh(k_2)h] \cdot \left[\frac{\omega_{(k_1)}\omega_{(k_2)}k_i \tanh k_i h}{\omega_{(k_i)}k_1 k_2 \tanh k_1 h \tanh k_2 h} \right]^{1/2} \right\}, \quad (1c)$$

$$\bar{W}_{(\mathbf{k}_i, \mathbf{k}_1, \mathbf{k}_2, \mathbf{k}_3)} = \bar{W}_{(-\mathbf{k}_i, -\mathbf{k}_1, \mathbf{k}_2, \mathbf{k}_3)} + \bar{W}_{(\mathbf{k}_2, \mathbf{k}_3, -\mathbf{k}_i, -\mathbf{k}_1)} - \bar{W}_{(\mathbf{k}_2, -\mathbf{k}_1, -\mathbf{k}_i, \mathbf{k}_3)} - \bar{W}_{(-\mathbf{k}_i, \mathbf{k}_2, -\mathbf{k}_1, \mathbf{k}_3)} - \bar{W}_{(-\mathbf{k}_i, \mathbf{k}_3, \mathbf{k}_2, -\mathbf{k}_1)} - \bar{W}_{(\mathbf{k}_3, -\mathbf{k}_1, \mathbf{k}_2, -\mathbf{k}_i)}, \quad (1d)$$

with

$$\bar{W}_{(\mathbf{k}_i, \mathbf{k}_1, \mathbf{k}_2, \mathbf{k}_3)} = \frac{1}{64\pi^2} \cdot \left[\frac{\omega_{(k_i)}\omega_{(k_1)}k_i k_1 k_2 k_3 \tanh(k_i)h \tanh(k_1)h \tanh(k_2)h \tanh(k_3)h}{\omega_{(k_2)}\omega_{(k_3)}} \right]^{1/2} \cdot \left[2 \left(\frac{k_i}{\tanh(k_i)h} + \frac{k_1}{\tanh(k_1)h} \right) - \left| \mathbf{k}_1 + \mathbf{k}_3 \right| \tanh \left| \mathbf{k}_1 + \mathbf{k}_3 \right| h - \left| \mathbf{k}_1 + \mathbf{k}_2 \right| \tanh \left| \mathbf{k}_1 + \mathbf{k}_2 \right| h - \left| \mathbf{k}_i + \mathbf{k}_3 \right| \tanh \left| \mathbf{k}_i + \mathbf{k}_3 \right| h - \left| \mathbf{k}_i + \mathbf{k}_2 \right| \tanh \left| \mathbf{k}_i + \mathbf{k}_2 \right| h \right]. \quad (1e)$$

The resonant conditions, as given by *Phillips* [1960], are

$$\mathbf{k}_3 = \mathbf{k}_i + \mathbf{k}_1 - \mathbf{k}_2, \quad \omega_{(\mathbf{k}_i)} + \omega_{(\mathbf{k}_1)} = \omega_{(\mathbf{k}_2)} + \omega_{(\mathbf{k}_3)}, \quad (2)$$

which are represented by the delta functions in (1a). These limit part of the integral to a contour, the so-called locus of interaction, thereby effectively reducing its dimensions. Following *Webb* [1978], *Tracy and Resio* [1982], and *Resio and Perrie* [1991], we let $OB(\mathbf{k}_1)$ equal the argument of the angular frequency delta function. Setting $OB(\mathbf{k}_1) = 0$, the two resonant conditions in (2) can then be combined into a single relation:

$$OB(\mathbf{k}_1) = 0 = \omega_{(\mathbf{k}_i)} + \omega_{(\mathbf{k}_1)} - \omega_{(\mathbf{k}_2)} - \omega_{(\mathbf{k}_i+\mathbf{k}_1-\mathbf{k}_2)}, \quad (3)$$

Introducing (\mathbf{n}, \mathbf{s}) coordinates, normal and tangential to the interaction locus defined by (3), we may rewrite (1a) as

$$\frac{\partial A_{(\mathbf{k}_i)}}{\partial \tau} = 4\pi \int_{-\infty}^{\infty} d\mathbf{k}_2 \left\{ \iint ds d\mathbf{n} [\delta[OB(\mathbf{s}, \mathbf{n})]] \right\} \cdot T_{i,1,2,3}^2 \{ A_{(\mathbf{k}_3)} A_{(\mathbf{k}_2)} [A_{(\mathbf{k}_i)} + A_{(\mathbf{k}_i)}] \}$$

$$- A_{(\mathbf{k}_i)} A_{(\mathbf{k}_i)} [A_{(\mathbf{k}_3)} + A_{(\mathbf{k}_2)}] \}. \quad (4)$$

The Dirac delta function has the following property [*Jackson*, 1962]:

$$\delta[f(x)] = \frac{\delta(x - x_0)}{\left| \frac{df}{dx} \right|}, \quad f(x_0) = 0,$$

which implies

$$\delta[OB(\mathbf{s}, \mathbf{n})] = \frac{\delta(\mathbf{n} - 0)}{\left| \frac{\partial OB(\mathbf{s}, \mathbf{n})}{\partial \mathbf{n}} \right|}. \quad (5)$$

Since $\int d\mathbf{n} [\delta(\mathbf{n} - 0)] = 1$, substituting (5) into (4), we obtain

$$\frac{\partial A_{(\mathbf{k}_i)}}{\partial \tau} = 4\pi \int_0^{\infty} dk_2 \int_0^{2\pi} d\theta \left[2 \oint ds \left| \frac{\partial OB(\mathbf{s}, \mathbf{n})}{\partial \mathbf{n}} \right|^{-1} \right] \cdot T_{i,1,2,3}^2 \theta_{(x)} \{ A_{(\mathbf{k}_3)} A_{(\mathbf{k}_2)} [A_{(\mathbf{k}_i)} + A_{(\mathbf{k}_i)}] - A_{(\mathbf{k}_i)} A_{(\mathbf{k}_i)} [A_{(\mathbf{k}_3)} + A_{(\mathbf{k}_2)}] \}, \quad (6)$$

where

$$\left| \frac{\partial OB(\mathbf{s}, \mathbf{n})}{\partial \mathbf{n}} \right| = \left| \frac{\partial [\omega_{k_1} - \omega_{(|\mathbf{k}_i - \mathbf{k}_2 + \mathbf{k}_1|)}]}{\partial k_{1x}} \hat{i} + \frac{\partial [\omega_{k_1} - \omega_{(|\mathbf{k}_i - \mathbf{k}_2 + \mathbf{k}_1|)}]}{\partial k_{1y}} \hat{j} \right|, \quad (7a)$$

and the Heaviside function is

$$\theta_{(x)} = 1 \quad x > 0, \quad (7b)$$

$$\theta_{(x)} = 0 \quad x < 0,$$

$$x = |\mathbf{k}_i - \mathbf{k}_3| - |\mathbf{k}_i - \mathbf{k}_2|.$$

Equation (6) reduces the original six-dimensional singular integration equation (1a) to a three-dimensional regular integration by eliminating two delta functions and evaluating the integral along a resonant orbit, as suggested by *Webb* [1978] and *Tracy and Resio* [1982].

The function $T_{i,1,2,3}$ in (6) is given by the (1b). The fifth and sixth terms in the right-hand side of the (1b):

$$\frac{1}{\omega_{(\mathbf{k}_i+\mathbf{k}_1)} - \omega_{(\mathbf{k}_i)} - \omega_{(\mathbf{k}_1)}} + \frac{1}{\omega_{(\mathbf{k}_2+\mathbf{k}_3)} - \omega_{(\mathbf{k}_2)} - \omega_{(\mathbf{k}_3)}},$$

$$\frac{1}{\omega_{(\mathbf{k}_2+\mathbf{k}_3)} + \omega_{(\mathbf{k}_2)} + \omega_{(\mathbf{k}_3)}} + \frac{1}{\omega_{(\mathbf{k}_i+\mathbf{k}_1)} + \omega_{(\mathbf{k}_i)} + \omega_{(\mathbf{k}_1)}},$$

are bound by the resonant conditions. However, the first four terms in the right-hand side of (1b) are not bound, because

$$\frac{1}{\omega_{(\mathbf{k}_1-\mathbf{k}_3)} - \omega_{(\mathbf{k}_3)} + \omega_{(\mathbf{k}_1)}} + \frac{1}{\omega_{(\mathbf{k}_2)} + \omega_{(\mathbf{k}_i-\mathbf{k}_2)} - \omega_{(\mathbf{k}_i)}} \xrightarrow{\mathbf{k}_i \rightarrow \mathbf{k}_2(\mathbf{k}_1 \rightarrow \mathbf{k}_3)} \infty.$$

This means that if $\mathbf{k}_i \rightarrow \mathbf{k}_2$ or $\mathbf{k}_1 \rightarrow \mathbf{k}_3$, the denominators of these quotients will approach zero. Therefore these parts will approach infinity. A similar explanation applies to the following formulations.

$$\frac{1}{\omega_{(\mathbf{k}_1-\mathbf{k}_3)} - \omega_{(\mathbf{k}_1)} + \omega_{(\mathbf{k}_3)}} + \frac{1}{\omega_{(\mathbf{k}_i)} + \omega_{(\mathbf{k}_2-\mathbf{k}_i)} - \omega_{(\mathbf{k}_2)}} \xrightarrow{\mathbf{k}_i \rightarrow \mathbf{k}_2(\mathbf{k}_1 \rightarrow \mathbf{k}_3)} \infty,$$

$$\frac{1}{\omega_{(\mathbf{k}_1-\mathbf{k}_2)} - \omega_{(\mathbf{k}_2)} + \omega_{(\mathbf{k}_1)}} + \frac{1}{\omega_{(\mathbf{k}_3)} + \omega_{(\mathbf{k}_3-\mathbf{k}_1)} - \omega_{(\mathbf{k}_1)}} \xrightarrow{\mathbf{k}_i \rightarrow \mathbf{k}_3(\mathbf{k}_1 \rightarrow \mathbf{k}_2)} \infty,$$

$$\frac{1}{\omega_{(\mathbf{k}_1-\mathbf{k}_2)} - \omega_{(\mathbf{k}_1)} + \omega_{(\mathbf{k}_2)}} + \frac{1}{\omega_{(\mathbf{k}_1)} + \omega_{(\mathbf{k}_3-\mathbf{k}_1)} - \omega_{(\mathbf{k}_3)}} \xrightarrow{\mathbf{k}_i \rightarrow \mathbf{k}_3(\mathbf{k}_1 \rightarrow \mathbf{k}_2)} \infty.$$

Therefore the nonlinear coefficient $T_{i,1,2,3}$ from (1a) is mainly determined by the limits $\mathbf{k}_i \rightarrow \mathbf{k}_2$ and $\mathbf{k}_1 \rightarrow \mathbf{k}_3$, in which case, the nonlinear transfer coefficient $T_{i,1,2,3}$ converges to $T_{i,1,i,3}$ and $T_{i,1,2,1}$ and we may write $T_{i,1,2,3} \approx T_{i,1,i,3} + T_{i,1,2,i}$. We can express \mathbf{k}_3 in terms of \mathbf{k}_2 by using resonant conditions, with \mathbf{k}_i and \mathbf{k}_1 fixed. Furthermore, from (7a), we see that if $\mathbf{k}_i \rightarrow \mathbf{k}_2$, then $|\partial OB/\partial n| \rightarrow 0$ and the right-hand side of (6) converges to its maximum. For these two reasons, we conclude that the nonlinear coefficient $T_{i,1,2,3}$ is mostly determined by contributions occurring when $\mathbf{k}_i \rightarrow \mathbf{k}_2$ and $\mathbf{k}_1 \rightarrow \mathbf{k}_3$. Therefore we do not need to integrate k_2 from 0 to ∞ , but only from $k_i - \Delta k$ to $k_i + \Delta k$. Equation (6) becomes

$$\frac{\partial A_{(\mathbf{k}_i)}}{\partial \tau} = 4\pi \int_{k_i-\Delta k}^{k_i+\Delta k} dk_2 \int_0^{2\pi} d\theta \left[2 \oint ds \left| \frac{\partial OB(\mathbf{s}, \mathbf{n})}{\partial n} \right|^{-1} \right] \cdot T_{i,1,2,3}^2 \theta_{(x)} \{ A_{(\mathbf{k}_3)} A_{(\mathbf{k}_2)} [A_{(\mathbf{k}_1)} + A_{(\mathbf{k}_i)}] - A_{(\mathbf{k}_1)} A_{(\mathbf{k}_i)} [A_{(\mathbf{k}_3)} + A_{(\mathbf{k}_2)}] \}. \quad (8)$$

where $k_i = |\mathbf{k}_i|$, and $\Delta k_i = \Delta |\mathbf{k}_i|$.

By optimizing accuracy and efficiency, through numerical tests (see appendix), we find associated values for Δk and $\Delta \theta$ ($\Delta \mathbf{k}$). As only very limited k_i domain ($k_i \pm \Delta k$) is involved in (8), we describe this integral as quasi-two dimensional. Therefore, we have reduced a three-dimensional integration (equation (6)) to a quasi-two-dimensional integration (equation (8)). In fact, we can further reduce the integration to a quasi-line integration, because the limitation on \mathbf{k} restricts the angle ($\Delta \theta$) of integration on \mathbf{k}_2 . However, when $\mathbf{k}_1 = \mathbf{k}_2$ and $\mathbf{k}_1 = \mathbf{k}_3$, the product of actions in (8) will vanish. We can solve this problem by finding θ'_i instead of θ_i , where the integration in (8) at a fixed θ is maximum. Thus we have finally,

$$\frac{\partial A_{(\mathbf{k}_i)}}{\partial \tau} = 4\pi \int_{k_i-\Delta k}^{k_i+\Delta k} dk_2 \int_{\theta'_i-\Delta \theta}^{\theta'_i+\Delta \theta} d\theta \left[2 \oint ds \left| \frac{\partial OB(\mathbf{s}, \mathbf{n})}{\partial n} \right|^{-1} \right] \cdot T_{i,1,2,3}^2 \theta_{(x)} \{ A_{(\mathbf{k}_3)} A_{(\mathbf{k}_2)} [A_{(\mathbf{k}_1)} + A_{(\mathbf{k}_i)}] - A_{(\mathbf{k}_1)} A_{(\mathbf{k}_i)} [A_{(\mathbf{k}_3)} + A_{(\mathbf{k}_2)}] \} \quad (9)$$

which constitutes the reduced integration approximation (RIA).

In the limit of a full integration, RIA is equal to SSM. This includes the computation of the loci, and the phase terms; however, the coupling coefficient of RIA is based on Hamiltonian formulation [Lin and Perrie, 1997], and those of SSM is based on modified Webb formulation [Trancy and Resio, 1982]. In the tests implemented in the next section, the integration limits on (9) are constrained by $\Delta \theta = 30^\circ$ and, in terms of frequency, $\Delta f = 0.4f_p$, where f_p is the spectral peak frequency.

3. Verification of RIA

In the above section we have examined the resonant domain analytically and reduced the six-dimensional integration to lower-dimensional integrations. In this section, we will numerically compare the original integration with the approximation integrations. To facilitate the comparison, we will use the same

JONSWAP spectrum with a narrow peak spreading (Hasselmann-Mitsuyasu spreading) as in LP97, which is shown in Figure 1a. We also use the Pierson-Moskowitz spectrum with wide angle spreading ($\cos^2 \theta$), as shown in Figures 1b, to simulate a fully saturated wave spectrum. Finally, Figure 1c uses the JONSWAP spectrum of Figure 1a, with $\cos^2 \theta$ spreading, as in Figure 1b. As mentioned above, we use linear dispersion.

Using the JONSWAP spectrum with Hasselmann-Mitsuyasu spreading of Figure 1a, we present the nonlinear transfer, in deep water in Figures 2a–2c. The nonlinear transfer of Figure 2a is computed by (6), which is a three-dimensional integration, whereas Figure 2b is computed using (8), which is a quasi-two dimensional integration, and Figure 2c is computed by (9), a quasi-line integral. In all these figures, the lines A, B, \dots , G represent the angles of action transfer from 0° , 30° , 60° , \dots , and 180° , respectively. As one can see, the shapes of each computation in Figures 2a–2c are similar. Similar results are presented in Figures 3a–3c, repeating the tests of Figures 2a–2c using an assumed Pierson-Moskowitz spectrum with $\cos^2 \theta$ spreading in finite depth conditions ($kh = 0.8$), following A. Masuda and K. Komatsu (manuscript in preparation, 1998) and Hashimoto *et al.* [1998].

To examine the variation in magnitude, we plot the one-dimensional action transfer, integrated over all the angles in Figures 4a and 4b. Lines A, B, and C, in Figures 4a and 4b represent the results from the full integration of (6), the two-dimensional approximation of (8), and the quasi-linear approximation of (9), respectively. Figure 4a gives results from the JONSWAP nonlinear transfers of Figure 2, whereas Figure 4b gives the results from the Pierson-Moskowitz nonlinear transfers of Figure 3. One can see that there is only a slight change in their magnitudes. The result obtained from the quasi-two dimensional integration is almost the same as that corresponding to the three-dimensional integration. Their maximal and minimal values differ from the values obtained from the quasi-line integral by $<12\%$. Further sensitivity tests are presented in the appendix. In the next section we compare RIA with the other nonlinear transfer formulations considered in this study.

4. Comparing RIA and Other Formulations

The tests of this section assume that (1) narrow peak spectra with Hasselmann-Mitsuyasu spreading, as shown by the JONSWAP parameterizations of Figure 1a, (2) widely spread old spectra, as shown by the Pierson-Moskowitz parameterizations of Figure 1b with $\cos^2 \theta$ spreading, and (3), widely spread young spectra, as shown by the JONSWAP parameterization of Figure 1c with $\cos^2 \theta$ spreading. These input spectra are chosen as important representatives of real ocean wave spectra. Moreover, these input spectra correspond to published tests for the nonlinear transfer formulations considered in this study.

In the following calculations, the frequency increments are given by $df_i = 0.08f_{i-1}$, and the angular discretization ($D\theta$) is 7.5° . The number of frequency bands is 35, and the number of angular bands is 48. The one-dimensional action transfer rate is presented in Figures 5a–5b, calculated by the RIA method. The initial spectra are the narrow JONSWAP spectrum of Figure 1a and the broad Pierson-Moskowitz spectrum of Figure 1b, respectively. The lines A, B, C, and D represent $kh = 36.3, 1.58, 1.0$ and 0.8 , respectively.

Using the narrow JONSWAP spectrum of Figure 1a, we

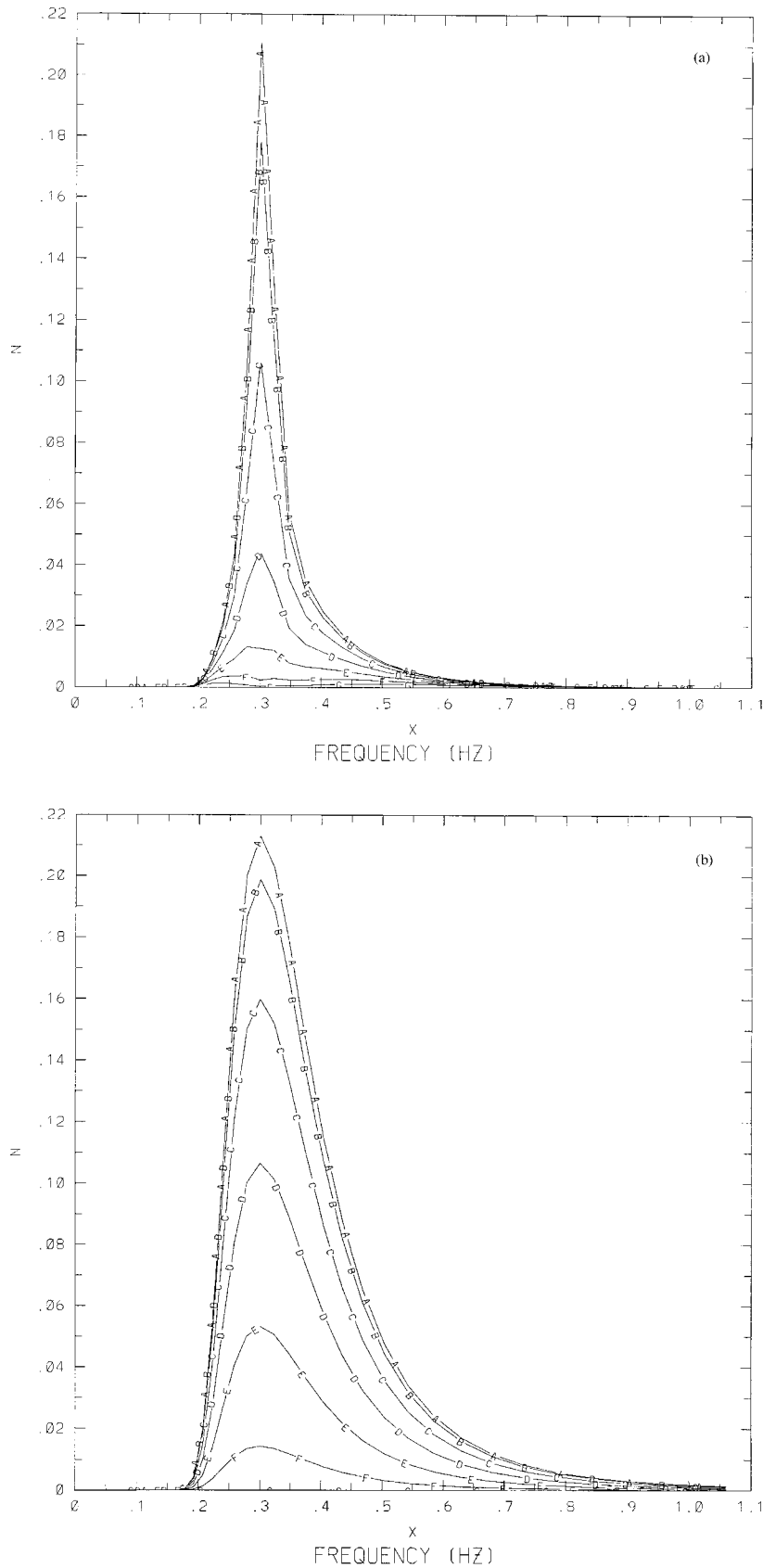


Figure 1. The initial input energy spectrum, where the energy density profile is given in 30° increments. The lines A, B, ..., G represent angles $0^\circ, 30^\circ, \dots, 180^\circ$. NCWM indicates the New Coastal Wave Model formulation for (6), as derived in LP97. (a) Using the JONSWAP spectrum, where $\sigma_a = 0.7$, $\sigma_b = 0.9$, $\gamma = 3.3$, $\alpha = 0.01$, and $f_p = 0.3$, with a Hasselmann-Mitsuyasu directional spreading distribution. (b) Pierson-Moskowitz spectrum with $\cos^2 \theta$ directional spreading. (c) As in Figure 1a, with $\cos^2 \theta$ spreading.

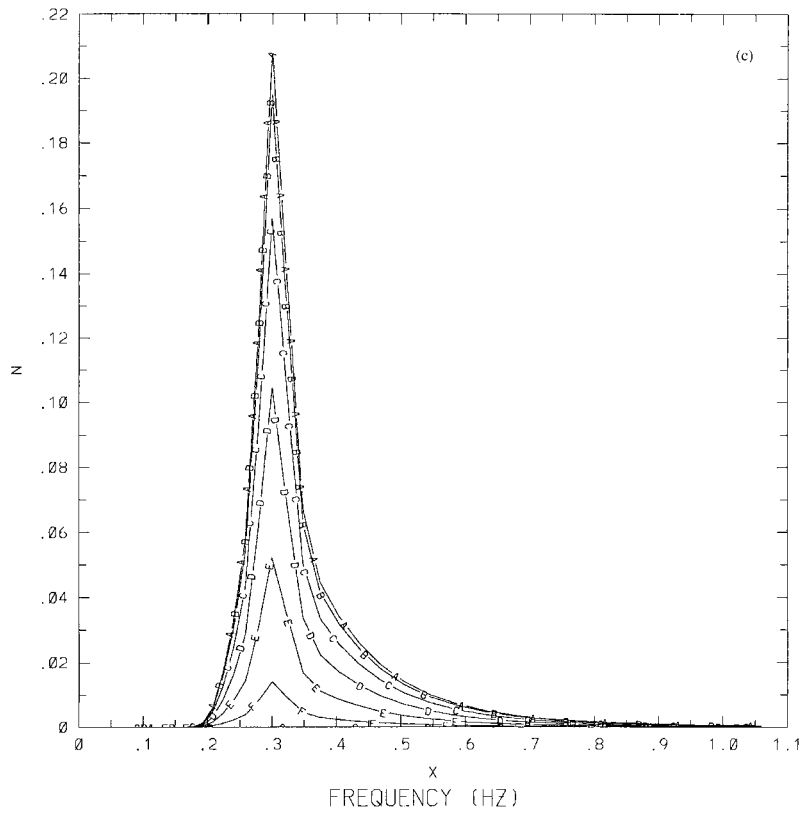
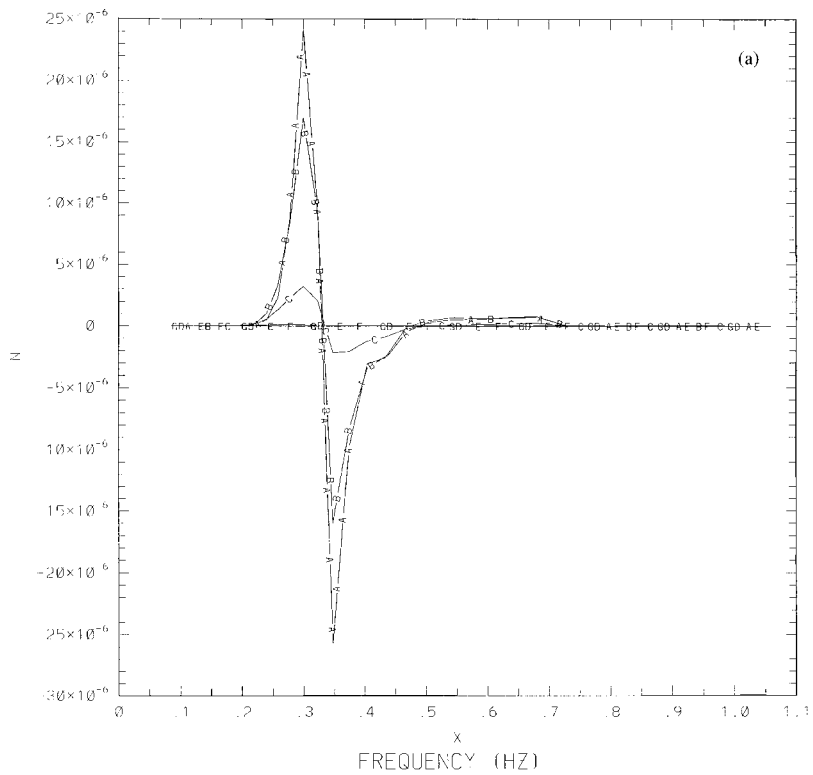
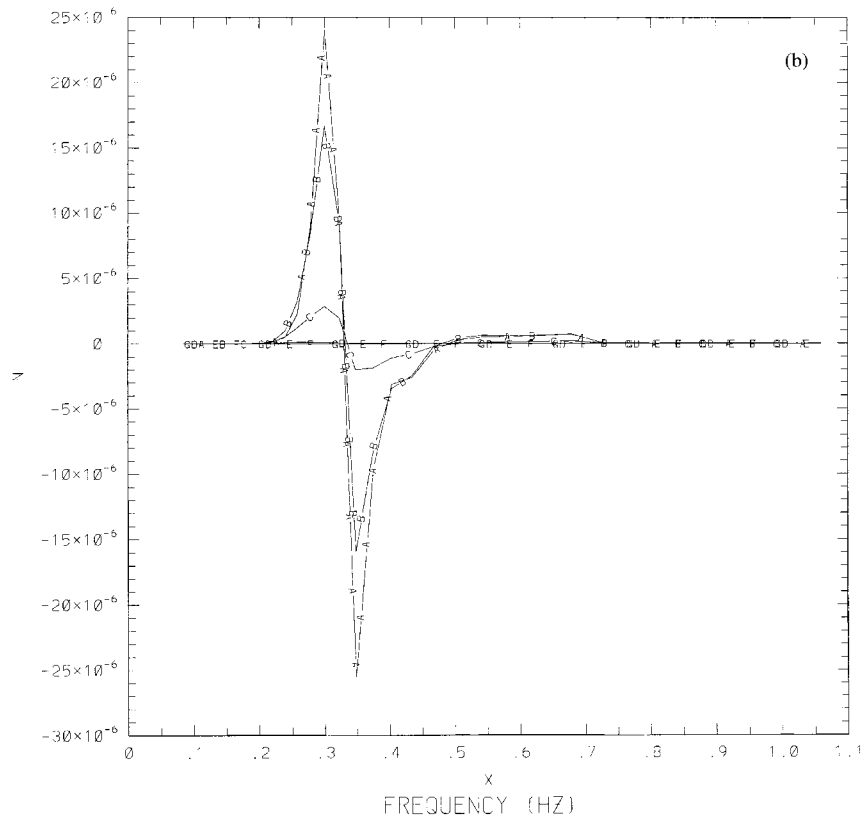


Figure 1. (continued)

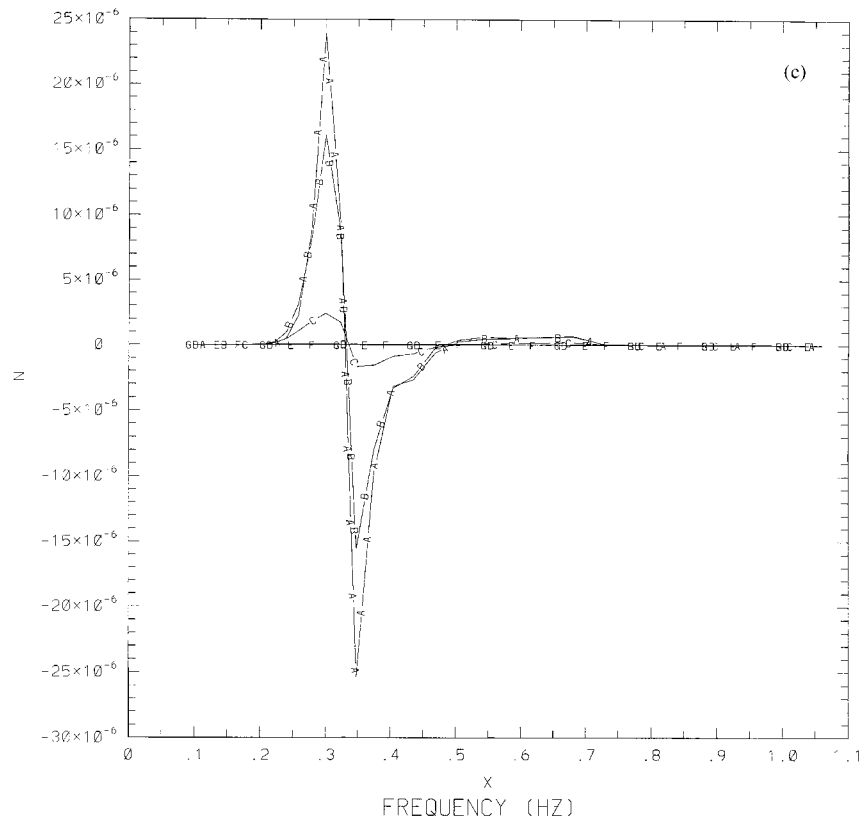


(NCWM, KH=36.3, LINEAR DISPERSION)

Figure 2. Comparisons of the various integration schemes for the nonlinear action transfer rate, using the initial spectrum of Figure 1a: (a) three-dimensional integration (equation (6)); (b) quasi-two dimensional integration (equation (8)); (c) quasi-line integration (equation (9)). The lines A, B, ..., G represent angles $0^\circ, 30^\circ, \dots, 180^\circ$. NCWM indicates the New Coastal Wave Model formulation for (6), as derived in LP97.

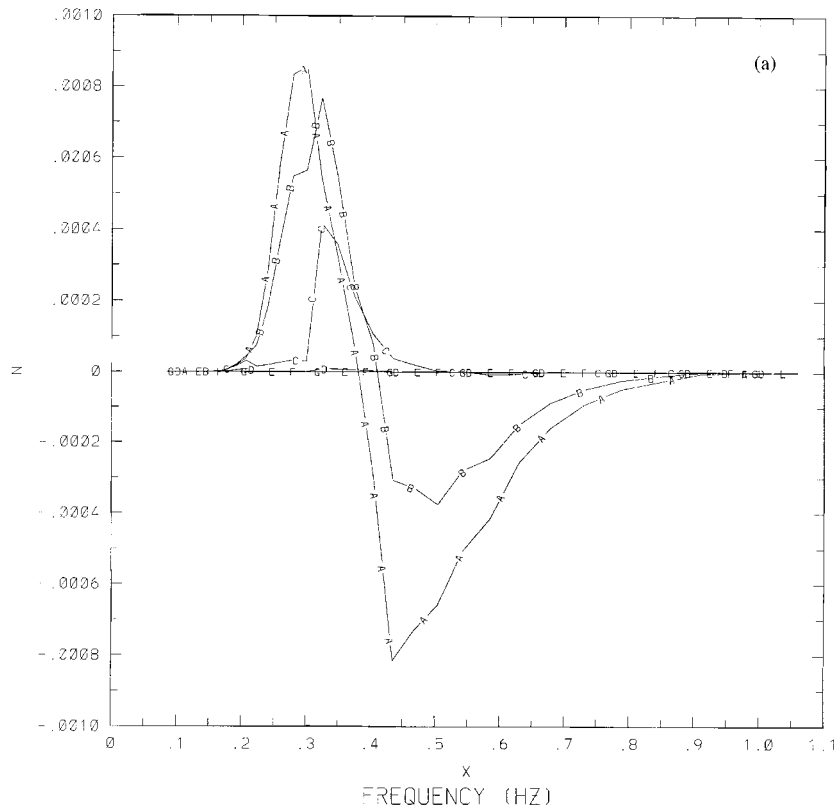


(NCWM, KH=36.3, LINEAR DISPERSION)

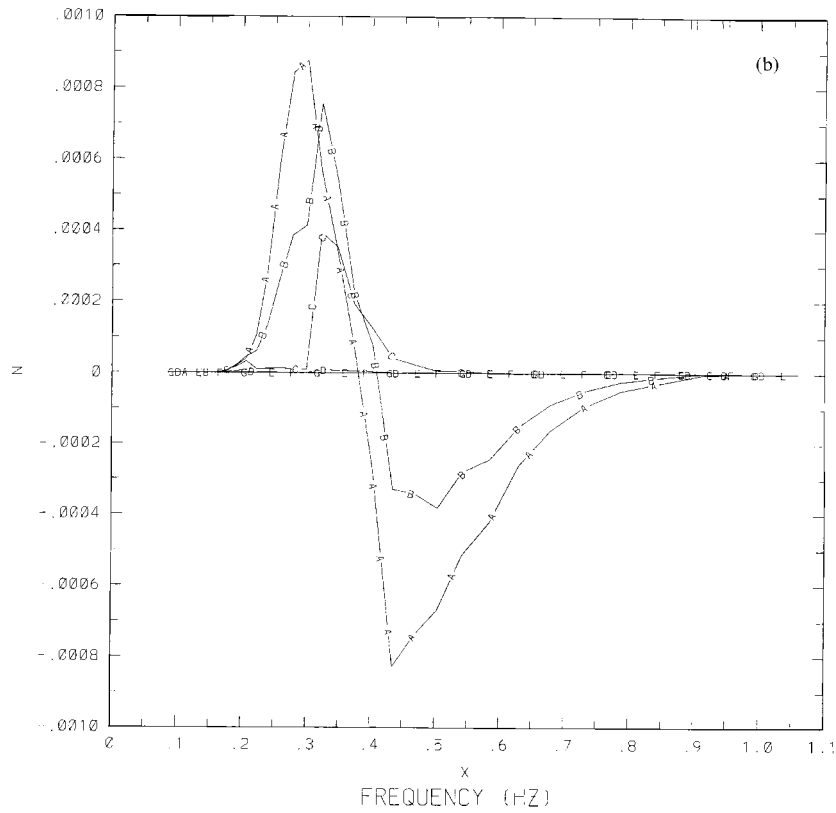


(NCWM, KH=36.3, LINEAR DISPERSION)

Figure 2. (continued)



(NCWM, KH=0.8, LINEAR DISPERSION)



(NCWM, KH=0.8, LINEAR DISPERSION)

Figure 3. Comparisons of the various integration schemes of the nonlinear action transfer rate using the initial spectrum of Figure 1b: (a) three-dimensional integration (equation (6)); (b) quasi-two dimensional integration (equation (8)); (c) quasi-line integration (equation (9)). The lines A, B, ..., G represent angles 0° , 30° , ..., 180° . NCWM indicates the New Coastal Wave Model formulation for (6), as derived in LP97.

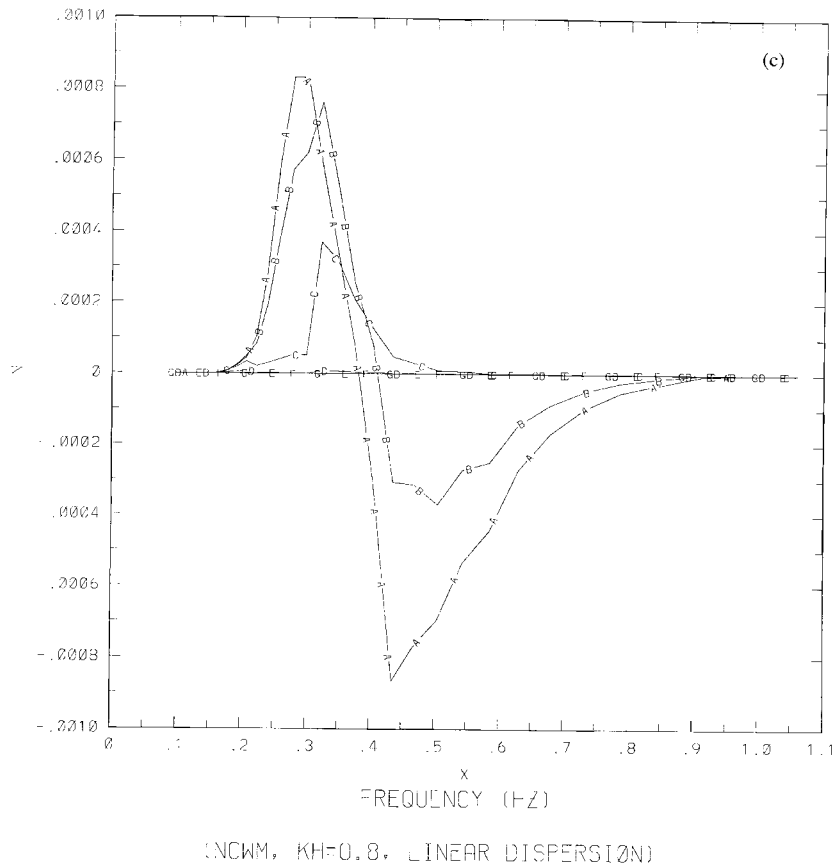


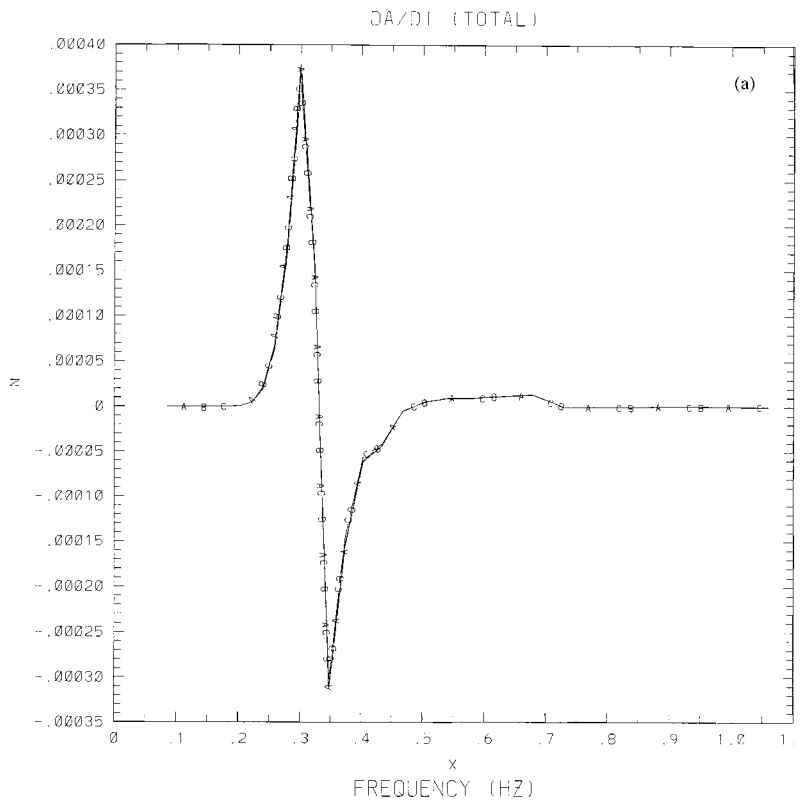
Figure 3. (continued)

show in Figure 5a that as the water depth decreases from deep to shallow, the nonlinear transfer rate initially decreases, until $kh \approx 1.58$. Thereafter, with further decreases in water depth, Figure 5a shows that the nonlinear transfer S_{nl} increases, in qualitative agreement with *Herterich and Hasselmann* [1980]. By comparison, the broad Pierson-Moskowitz spectrum of Figure 1b, leads to the nonlinear transfer shown in Figure 5b. This shows that the nonlinear transfer increases with decreasing water depth when $kh \geq 0.8$, which is in good quantitative agreement with A. Masuda and K. Komatsu (manuscript in preparation, 1998) and *Hashimoto et al.* [1998]. Finally, Figure 5c presents the nonlinear transfer resulting from the broad JONSWAP initial spectrum of Figure 1c. This shows that the nonlinear transfer increases with decreasing water depth in qualitative agreement with Figure 5b. Results from A. Masuda and K. Komatsu (manuscript in preparation, 1998) are given in Figure 5d, for $kh = 10.0$, 1.0 and 0.8. The nonlinear interactions are the same when $kh = 36.3$ or $kh = 10$, because they both are completely deep water cases. Figure 5d shows that the peak values of the nonlinear transfer at $kh = 0.8$ are 1.25 times the corresponding values at $kh = 1.0$, which is also consistent with similar figures by *Hashimoto et al.* [1998]. The change in scales between Figures 5b and 5c is about $5\times$, with is in good quantitative agreement with Figures 4a and 4b in *Hashimoto et al.* [1998]. This quantitative agreement becomes more evident when Figures 5b and 5c are normalized.

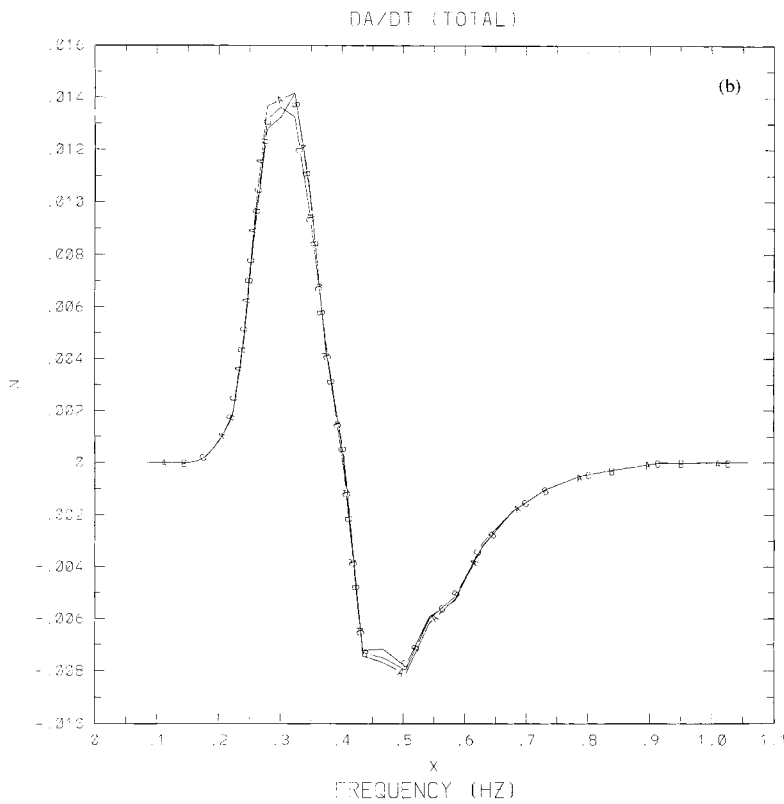
We have demonstrated, in the previous section and in this section, that the one-dimensional nonlinear action transfer, as estimated by the RIA method verifies well with more compre-

hensive full integral tests given in (6) and (8), and with accepted results from other research efforts, independent of water depth or the spectral spreading function. In Figures 6a–6c, we present the associated two-dimensional nonlinear action transfer, with frequency (Hz) plotted on the abscissa and wave direction ω plotted on the ordinate. Figure 6a is from the full integration of (6), and qualitatively verifies well with similar results obtained by *Hasselmann and Hasselmann* [1981] and *Resio and Perrie* [1991]. Figure 6b is computed using the formulation of *Hasselmann and Hasselmann* [1981]. Figure 6c is obtained from the formulation of *Resio and Perrie* [1991]. One can see that all the results are qualitatively very similar. The corresponding RIA integration is presented in Figure 7, and compares well with Figures 6a–6c, although the computation time is much smaller. For example, compared to the *Hasselmann and Hasselmann* [1981] formulation of Figure 6b, the computation time is several orders of magnitude faster.

The nonlinear transfer formulation originally proposed by *Zakharov* [1968] was for deep water only, whereas the formulation by *Hasselmann* [1962] includes finite depth water. However, the latter is based on the deep sea theory of *Crawford et al.* [1981], using the small perturbative parameter $\varepsilon \equiv ak$, where a is the wave amplitude. In LP97, we applied *Zakharov's* approximation to finite depth water and derived a formulation in terms of the global perturbative parameter $[ak(3 + \tanh^2 kh)]/(4 \tanh^3 kh)$. Our formulation also includes an appropriate nonlinear dispersion relationship. We showed that as the water becomes shallow, Phillips mechanics become less effective, the resonant condition involves three gravity waves

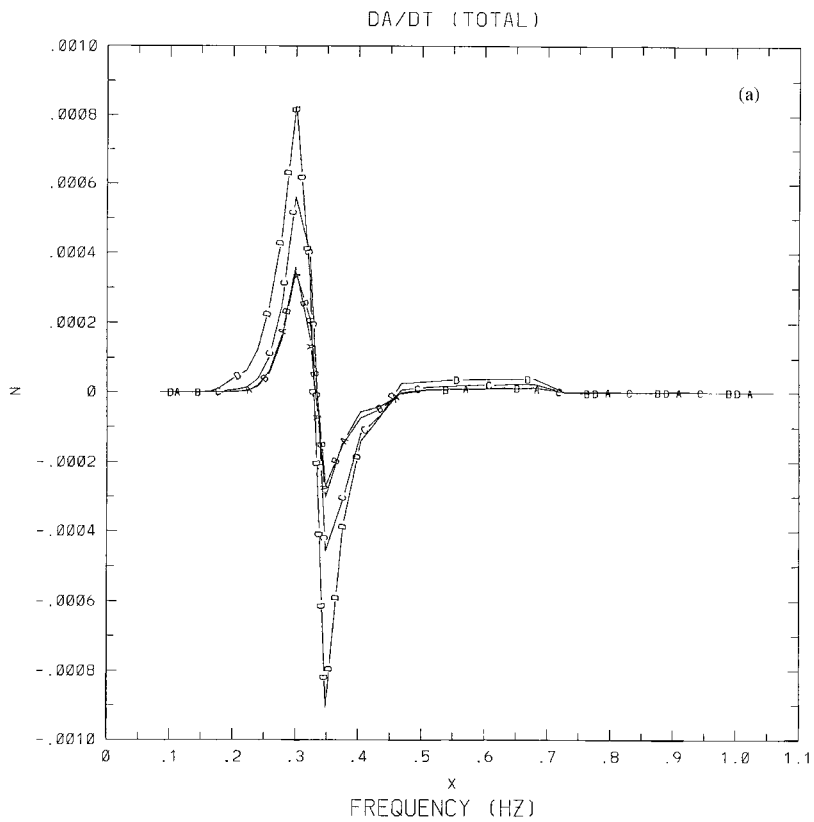


(KH=36.3, LINEAR DISPERSION)

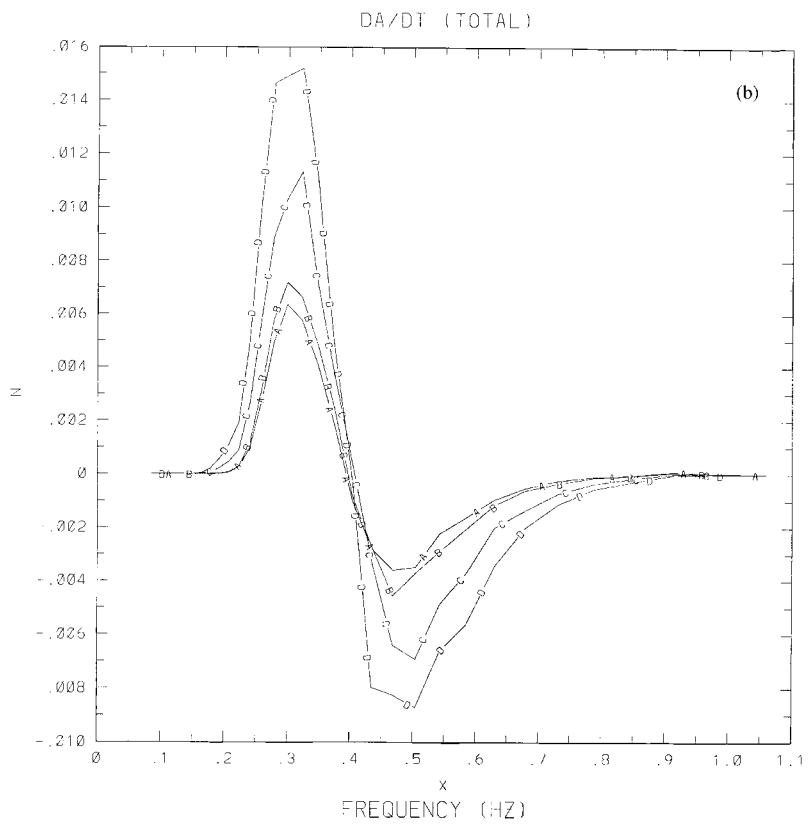


(KH=0.8, LINEAR DISPERSION)

Figure 4. Comparison of one-dimensional nonlinear action transfer rate integrated over all angles with various integration schemes, where lines A, B, and C represent (6), (8), and (9) respectively; (a) the initial spectrum of Figure 1a; (b) the initial spectrum of Figure 1b.

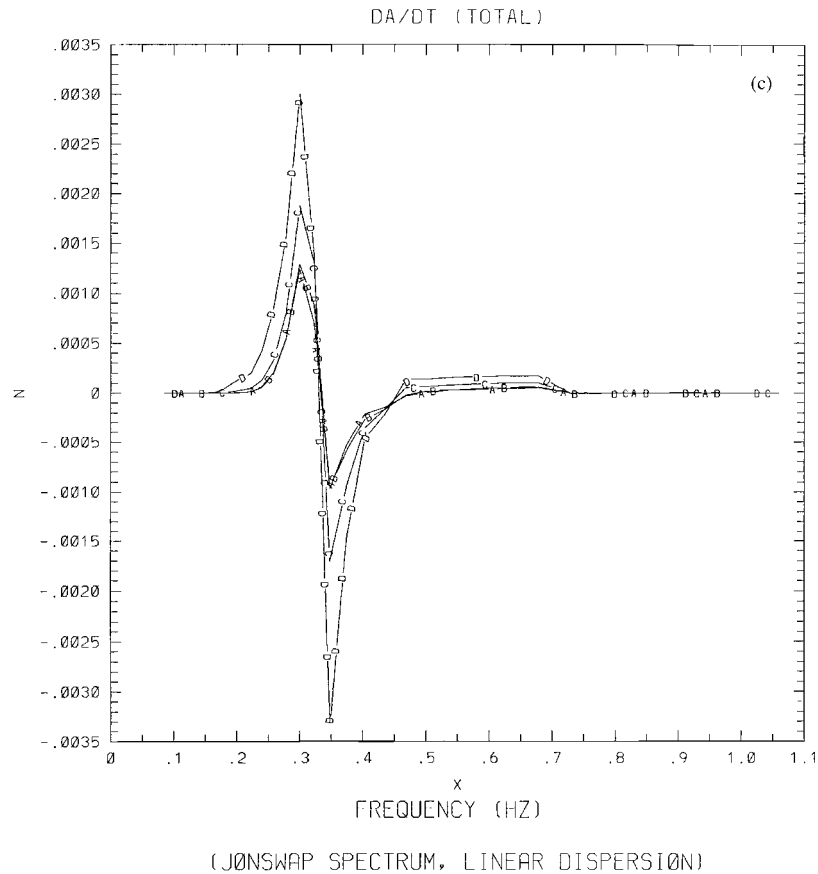


(JØNSRAP SPECTRUM, LINEAR DISPERSION)



(P-M SPECTRUM, LINEAR DISPERSION)

Figure 5. One-dimensional nonlinear transfer rate, where lines A, B, C, and D represent $kh = 36.3$ (10.0), 1.58, 1.0, and 0.8; (a) initial spectrum of Figure 1a; (b) initial spectrum of Figure 1b; (c) initial spectrum of Figure 1c; (d) from Masuda and Komatsu (manuscript in preparation, 1998) using Pierson-Moskowitz spectrum and $\cos^2 \theta$ directional spreading (with permission).



(JONSWAP SPECTRUM, LINEAR DISPERSION)

Figure 5. (continued)

interacting with one long wave and the nonlinear transfer rate is reduced, especially in very shallow water. In the deep water limit, our result is identical to that obtained from the *Zakharov* [1968] formulation.

A quantitative comparison of these formulations is given in Figure 8a, showing the maximal positive nonlinear transfer rates summed over all angles, plotted as a function of angular discretization sizes. It should be noted that as this is a very “sharp” peak, this constitutes a very sensitive measure of con-

sistency. In Figure 8, lines A, B, C, and D represent the methods by Lin-Perrie, Hasselmann and Hasselmann, Resio-Perrie, and RIA respectively. Figure 8 shows that the quantitative differences among the different formulations are due to the numerical computation. In fact, *Dyachenko and Lvov* [1994] have shown that the formulations by Zakharov and Hasselmann are analytically identical, for the one-dimensional case, and semianalytically identical, for the two-dimensional case. In our spectral computation, we found that the difference between formulations by *Hasselmann and Hasselmann* [1981], and Lin-Perrie is <8% and between Resio-Perrie and Lin-Perrie formulations, is 9.7%, if $D\theta \leq 7.5^\circ$. The differences increase drastically for $D\theta > 7.5^\circ$. Among all the formulations, the one by Hasselmann and Hasselmann is the most sensitive to the angular discretization size when $D\theta > 7.5^\circ$. To show this in another way, we also plotted the net nonlinear transfer, which is the total integral of DA/Dt over the entire frequency and direction domains, in Figure 8b. Since nonlinear wave-wave interactions are a conservative process, the net nonlinear transfer should be zero. However, because numerical computational errors accumulate throughout the calculation, all formulations show a rapid deterioration of action conservation as the angular discretization increases. This becomes a serious problem when $D\theta > 7.5^\circ$ as shown in Figure 8b, with curves identified as in Figure 7a. Therefore a wave model should always keep the angular discretization $<7.5^\circ$, regardless what formulation is used for nonlinear transfer.

It is important to note that EXACT-NL and related formulations are not “exact” because they do not represent analytical

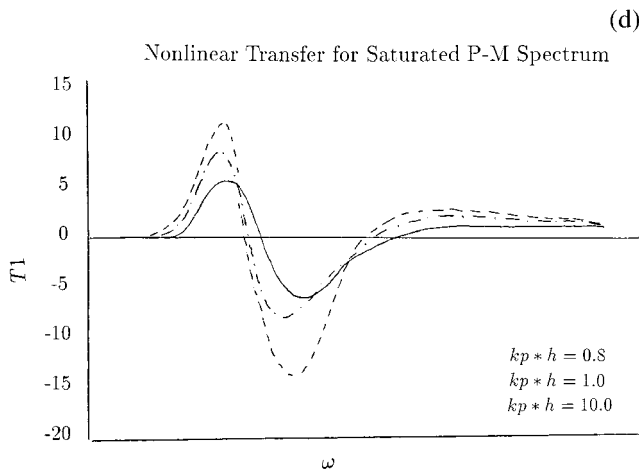


Figure 5. (continued)

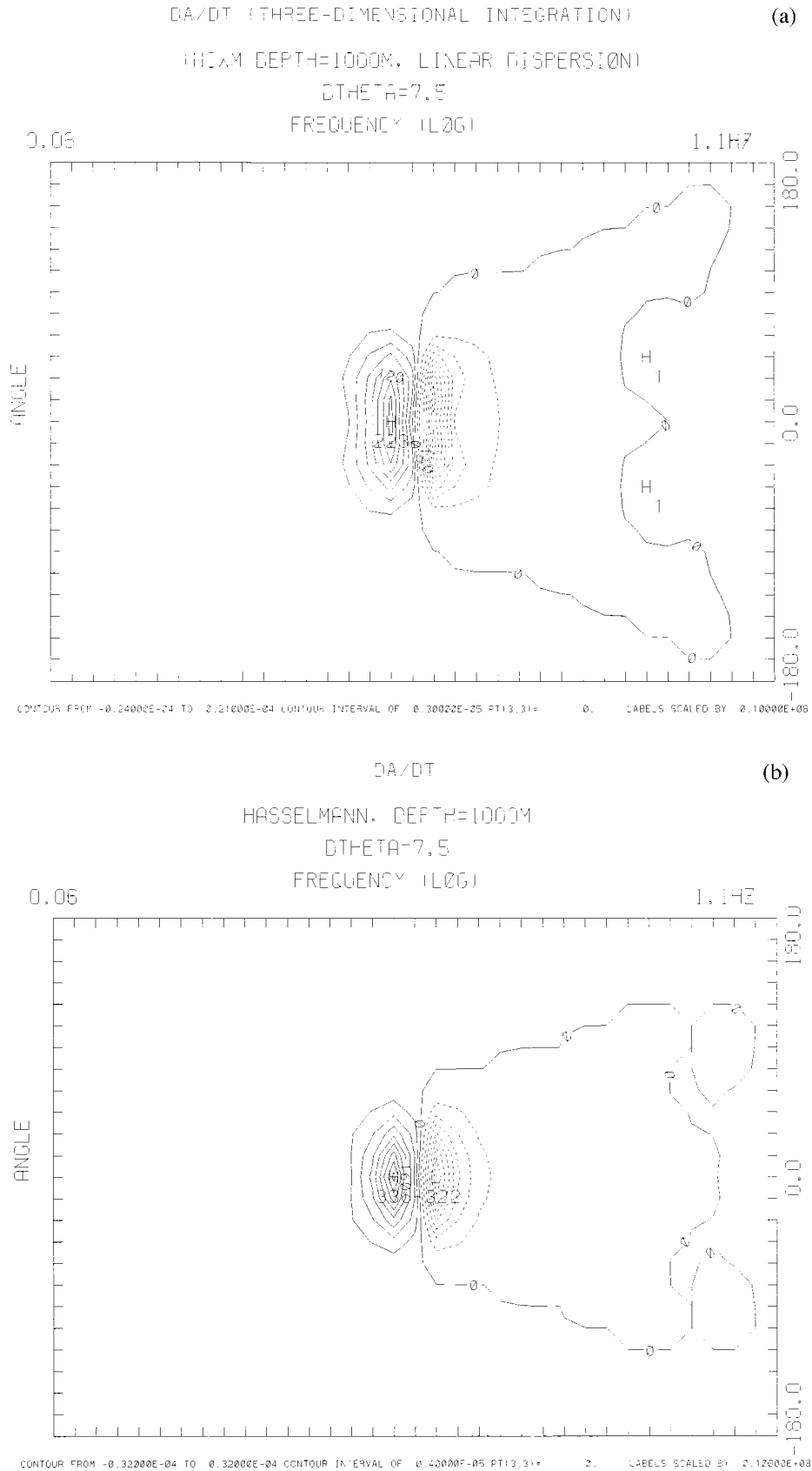


Figure 6. The full integral of the nonlinear action transfer from wave-wave interactions over deep water with linear dispersion; (a) from (6) ($kh = 36.3$) in frequency and direction coordinates. The increment between two contour lines is 3×10^{-6} ; (b) Hasselmann and Hasselmann [1985] formulation and (c) Resio and Perrie [1990] formulation. The increment between contour lines is 3×10^{-7} in Figure 6a and 3×10^{-6} in Figures 6b and 6c.

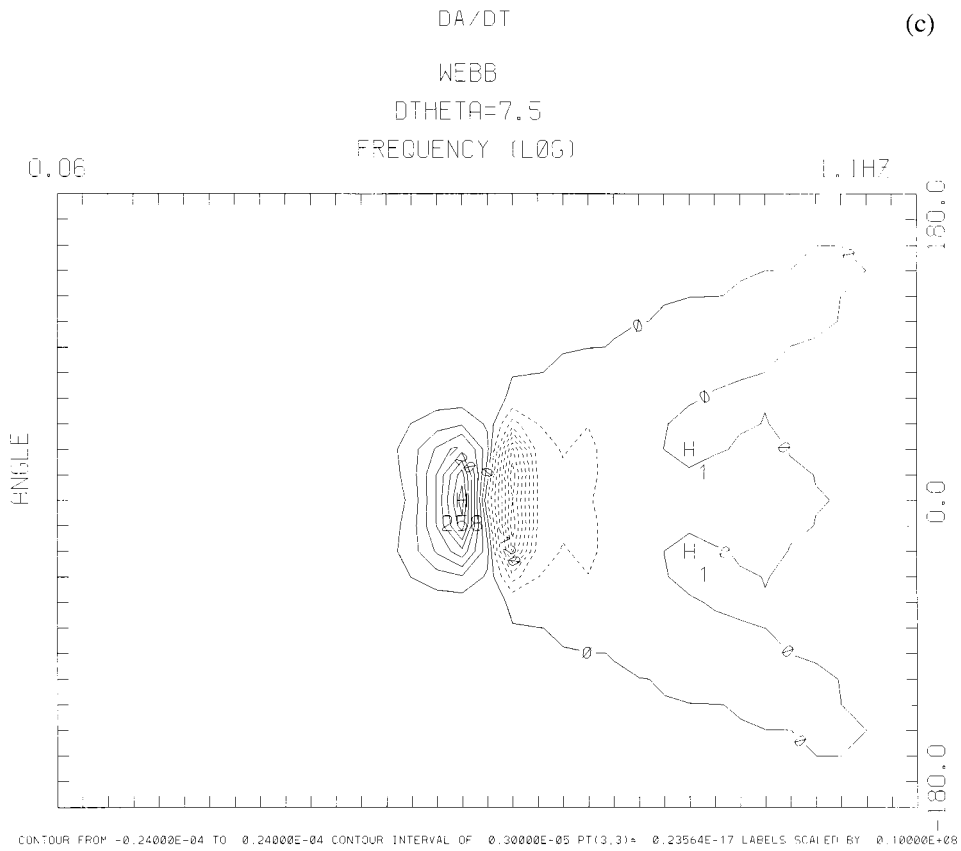


Figure 6. (continued)

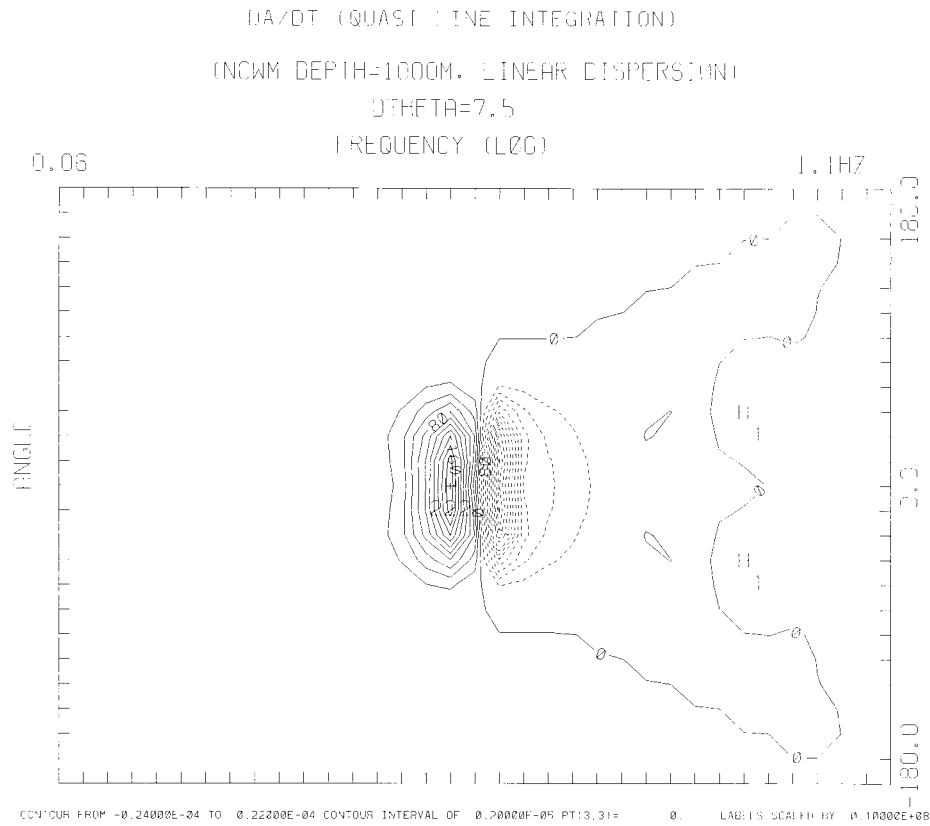


Figure 7. The nonlinear action transfer rate computed from the reduced integration approximation, RIA in (9). The increment between the contour lines is the same as in Figure 6a.

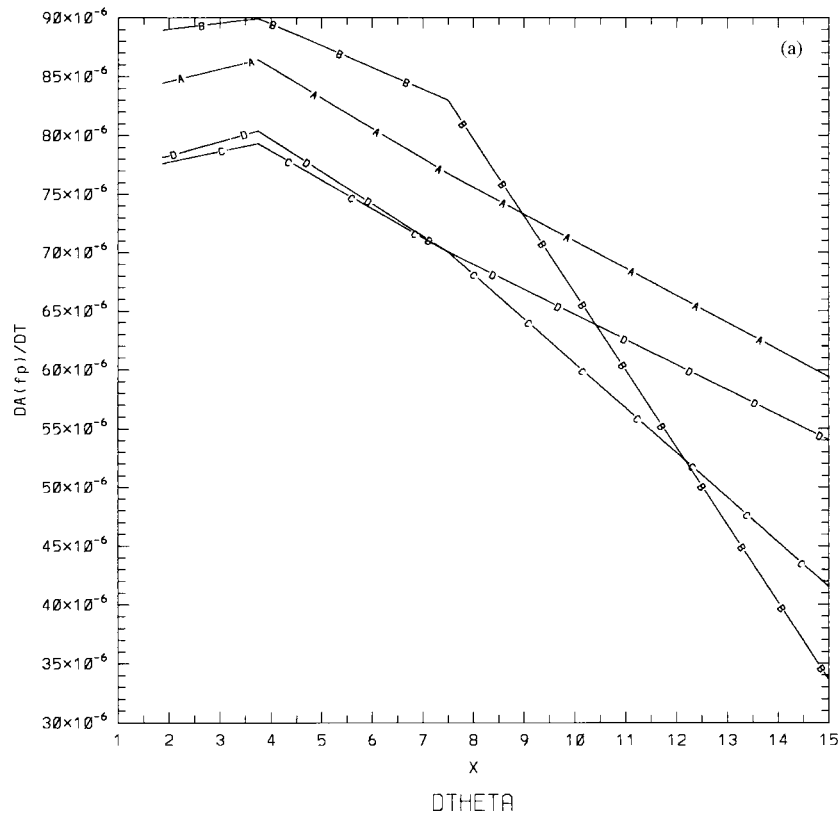


Figure 8a. Comparison of the maximal positive values summed over all angles, denoted $DA(fp)/DT$, where f_p is the peak frequency of the transfer rate, from various formulations, as a function of angle discretization: where A, B, C, and D represent Lin-Perrie, Hasselmann and Hasselmann, Resio-Perrie, and RIA.

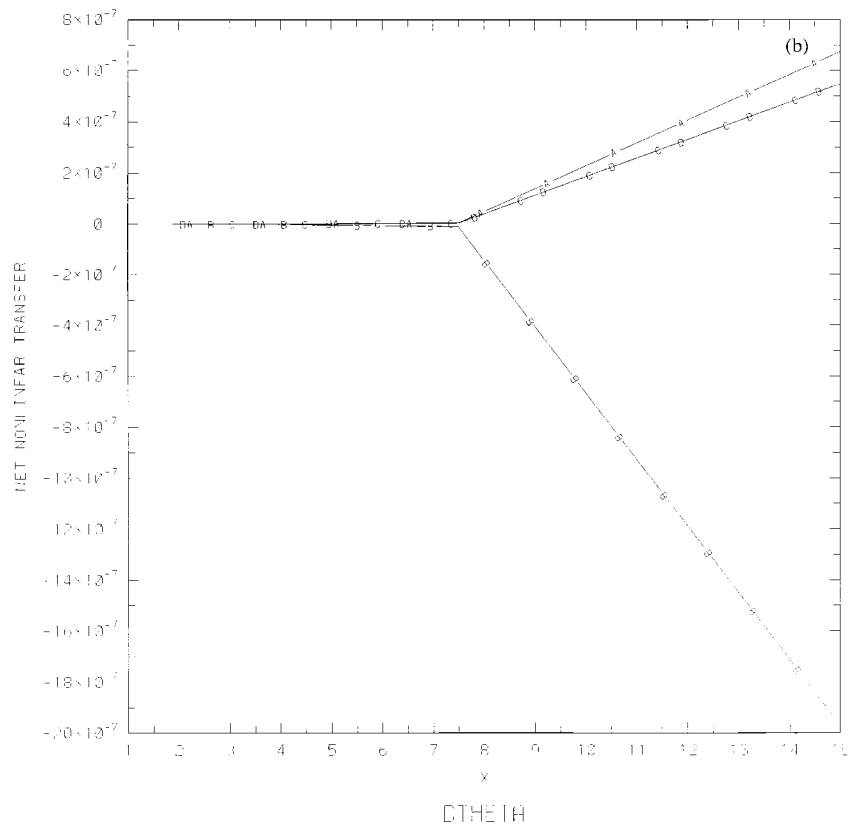


Figure 8b. Comparison of the net nonlinear transfer from various formulations as a function of angle discretization: where A, B, C, and D are the same as Figure 8a.

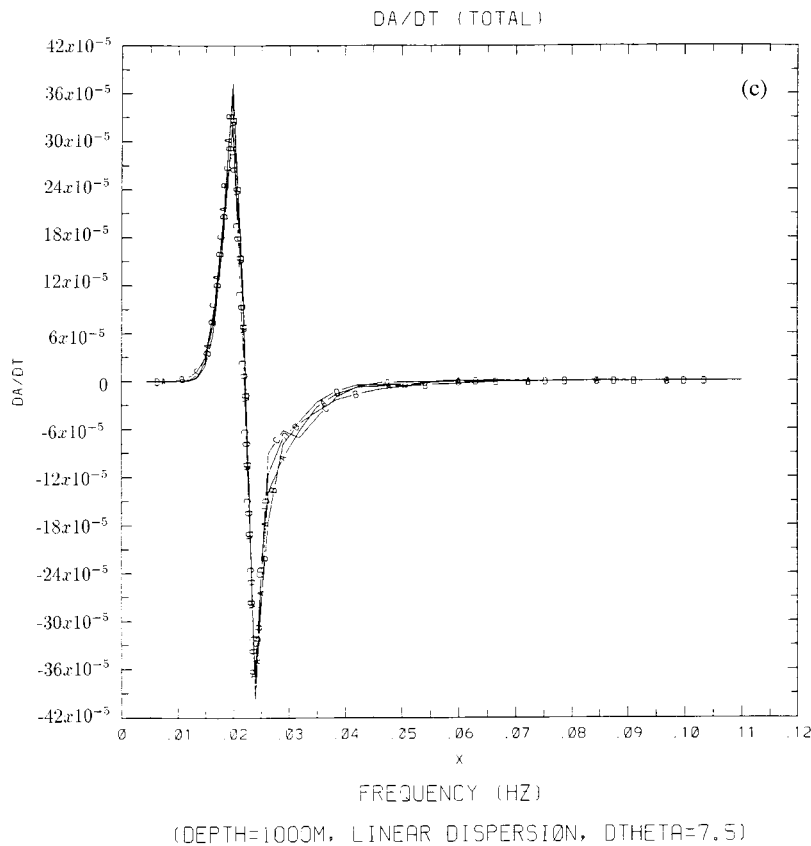


Figure 8c. Total action transfer rates summed over all angles in deep water, assuming linear dispersion and $D\theta = 7.5^\circ$. Line A represents Zakharov [1968] and Lin and Perrie's formulation of (6). Line B represents the Hasselmann and Hasselmann [1981] (EXACT-NL) formulation. Line C represents the Resio and Perrie [1990] formulation. Line D is calculated by the RIA formulation of (9).

calculations; they are only numerical computations. Of course, integrations involving higher resolutions are closer to the real solutions than integrations resulting from lower resolutions, especially because the resonant solutions have highly nonlinear distributions [Phillips, 1960]. Therefore calculations resulting from lower resolution integrations may not even follow the basic principles of the equation, such as conservation of energy. Figure 8b shows the relation between resolution and energy conservation for the numerical integrational methods considered in this study.

We compare the action transfer rates summed over all angles, from Lin and Perrie, Hasselmann and Hasselmann, Resio and Perrie, and RIA formulations, when $D\theta = 7.5^\circ$, in Figure 8c. The lines A, B, C, and D represent Lin and Perrie, Hasselmann and Hasselmann, Resio and Perrie, and RIA, respectively. Despite the differences in formulations, the overall action transfer rates still look very similar. One can see that they almost overlap. The maximum difference between these formulations is $<10\%$ at the peaks.

5. Conclusions

The RIA method is based on limiting the computational domain, as suggested by an analysis of coupling coefficient only. In this sense there is a difference between RIA and the EXACT-NL formulation, in which the computational domain is filtered on the basis of the small contributions to the total

integral, which are based on the product of the coupling coefficient, for a certain interaction, and the wave number product. In EXACT-NL, because the wave number product is needed, the filtering depends on the actual spectrum for which the nonlinear interactions are computed. In RIA, the "filtering" or "reduction" of the integration space does not depend on any target spectrum. This is an important difference.

In deep water, we have shown that the nonlinear transfer computed by RIA compares well with results obtained from the formulations by Hasselmann and Hasselmann [1981], Resio and Perrie [1991], and Lin and Perrie [1997]. In shallow water, RIA compares well with results from Herterich and Hasselmann [1980], Polnikov [1997], A. Masuda and K. Komatsu (manuscript in preparation, 1998), and Hashimoto *et al.* [1998]. In the deep water tests, we used JONSWAP spectrum with narrow spreading distribution (Hasselmann-Mitsuyasu) as input spectrum, as is used by Hasselmann and Hasselmann [1981], Resio and Perrie [1991], and Lin and Perrie [1997]. In the shallow water tests, we used Pierson-Moskowitz and JONSWAP spectra with a broad angular distribution ($\cos^2 \theta$), as is used by A. Masuda and K. Komatsu (manuscript in preparation, 1998) and Hashimoto *et al.* [1998]. This is important because the nonlinear transfer is very sensitive to the shape of the spectrum and the angular resolution, as noted by Hasselmann *et al.* [1985], as well as the water depth [Herterich and Hasselmann, 1980]. In these tests, we have shown that RIA

works well with the symmetric JONSWAP and PM spectra. In fact, RIA also works well with the directional sheared spectra [Jensen *et al.*, 1998].

In obtaining our results, we found that that RIA is only ~20 times slower than DIA, when its resolution consists of 35 frequency bands and 48 angle bands and DIA's resolution consists of 27 frequency bands and 12 angle bands. Therefore RIA is very efficient. This efficiency is several orders of magnitude faster than the other nonlinear transfer formulations, for example EXACT-NL. This makes RIA a very practical formulation, in view of its accuracy, particularly for operational shallow water modelling. However, the good RIA verifications we obtained in this study may depend on the tuning implicit in RIA (namely the selection for Δk and $\Delta\theta$). A final assessment of RIA must be based on further tests and comparisons, involving comprehensive wave model implementations, using both analytical spectral such as the SWAMP tests of Hasselmann *et al.* [1985], as well as real data, in a broad variety of spectral conditions. In computer tests, additional spectral forms, besides the JONSWAP and Pierson-Moskowitz spectra used here, must be involved.

Appendix

To compare the full Lin-Perrie formulation, given in (6), to the quasi-two dimensional integral in (8), we plot the nonlinear transfer DA/DT as a function of Δk in Figure A1, expressing

$k_i + \Delta k$ in terms of frequency, $f(k_i) \pm \Delta f$. The comparison uses $\Delta f = 1.10 \text{ Hz}$, $0.8f_p$, $0.4f_p$, $0.3f_p$. Sensitivity is minor until Δf is about $\leq 0.3f_p$. The difference in peak maximum values is ~10%. To test the sensitivity to $\Delta\theta$, we present DA/DT as a function of $\Delta\theta$ in Figure A2. Minor sensitivity is apparent when $\Delta\theta \leq 30^\circ$. The difference in peak maximum values is about 14%.

A more critical evaluation of RIA is given by consideration of the two-dimensional nonlinear transfer. Thus we present computations showing the sensitivity of DA/DT to Δf and $\Delta\theta$ in Figures A3–A5. Although the approximation to DA/DT presented in Figure A3 is slightly coarse, with $\Delta f = 0.3f_p$ and $\Delta\theta = 15^\circ$, it has the basic qualitative features displayed by complete integrations, as shown in Figure 6a (from equation (6)), Figure 6b from Hasselmann and Hasselmann and Figure 6c from Resio-Perrie. Figure A4, having $\Delta f = 0.3f_p$ and $\Delta\theta = 30^\circ$, more closely resembles the RIA formulation of Figure 7, and the other formulations of Figures 6. Finally, with $\Delta f = 0.4f_p$ and $\Delta\theta = 60^\circ$ in Figure A5, DA/DT goes beyond the RIA formulation and very closely matches the results presented in Figure 6a, and 6b and 6c for complete integrations.

It is important to emphasize that the results of Figures A1–A5 were achieved by using a fine resolution angle-frequency grid. A coarse grid would result in greatly reduced peak nonlinear transfer values. For example, using an angular discretization ($D\theta$) of 30° and frequency increments given by

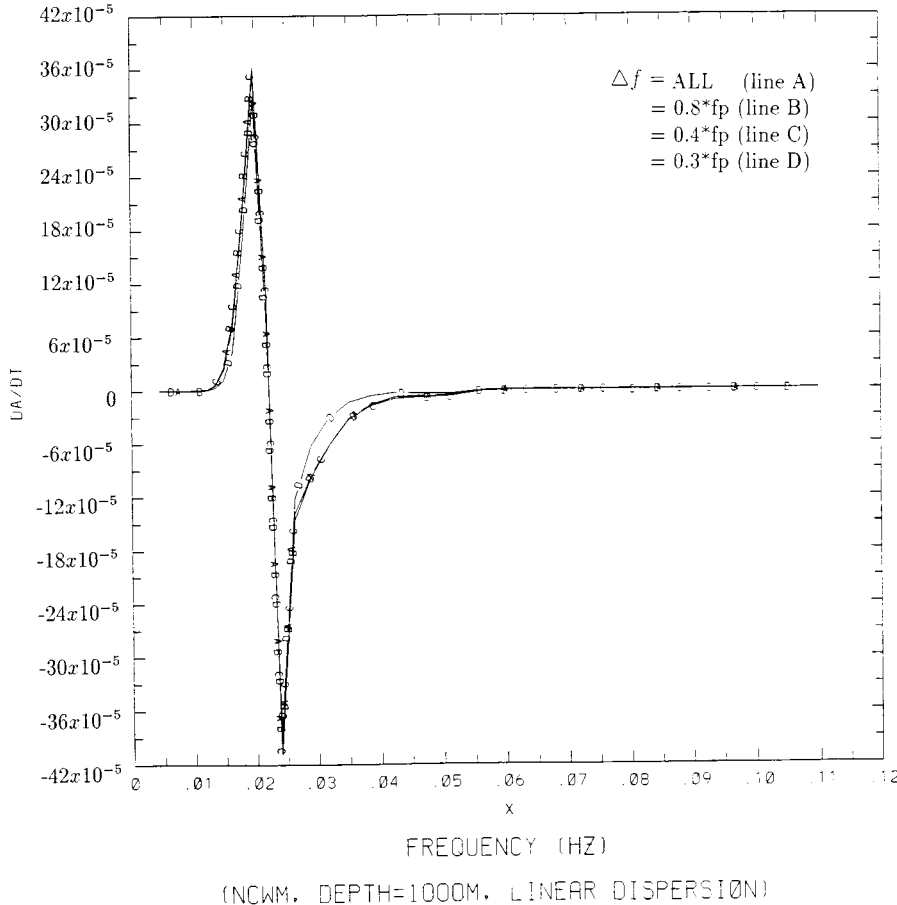
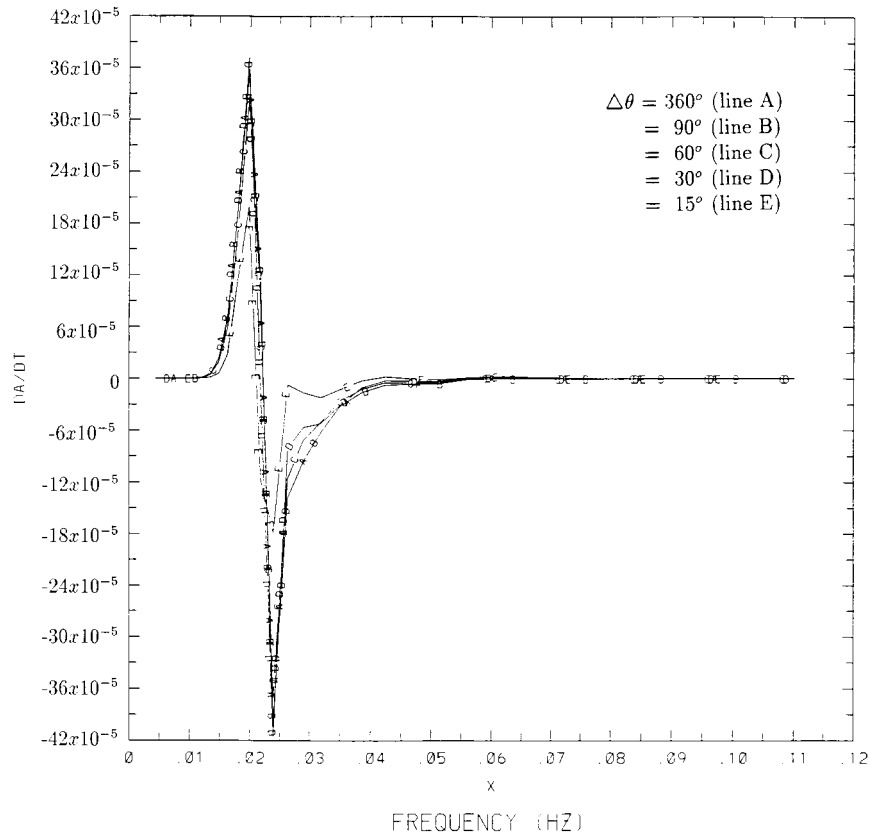


Figure A1. Total nonlinear transfer DA/DT as a function of Δk , expressing $k_i \pm \Delta k$ in terms of frequency $f(k_i) \pm \Delta f$, $\Delta f = 1.1 \text{ Hz}$, $0.8f_p$, $0.4f_p$, and $0.3f_p$.



(NCWM. DEPTH=1000M. LINEAR DISPERSION)

Figure A2. As in Figure A1, as a function of $\Delta\theta = 360^\circ, 90^\circ, 60^\circ, 30^\circ,$ and 15° .

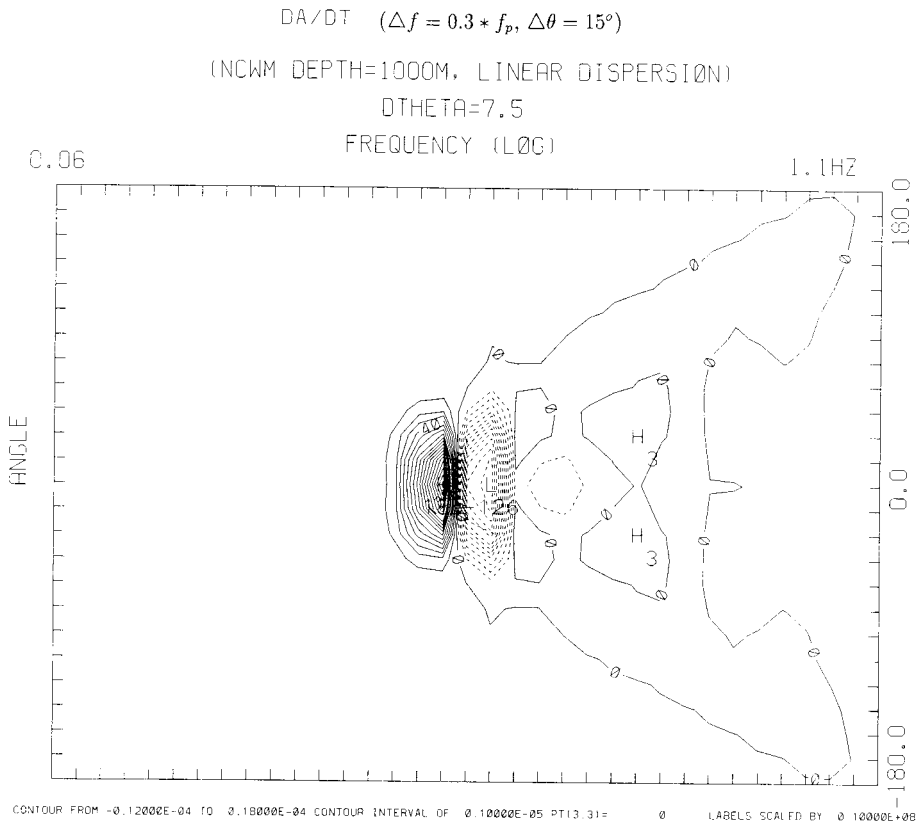


Figure A3. The two dimensional nonlinear transfer DA/DT , for an RIA formulation with $\Delta f = 0.3f_p$ and $\Delta\theta = 15^\circ$.

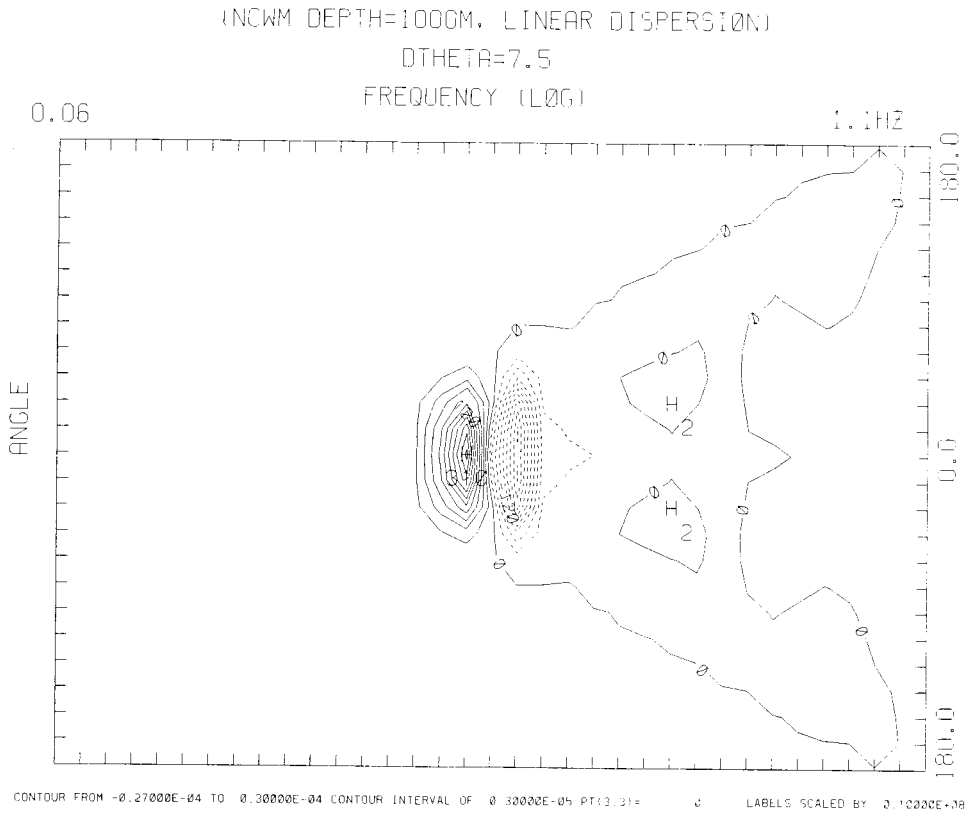


Figure A4. As in Figure A3 with $\Delta f = 0.3f_p$ and $\Delta\theta = 30^\circ$.

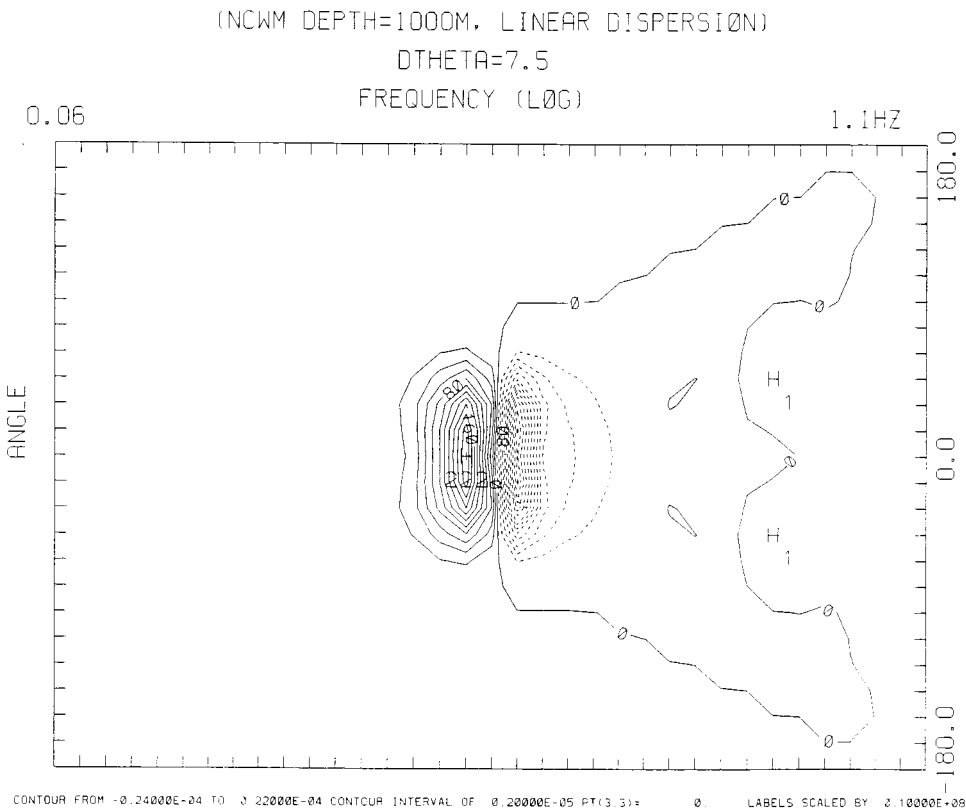
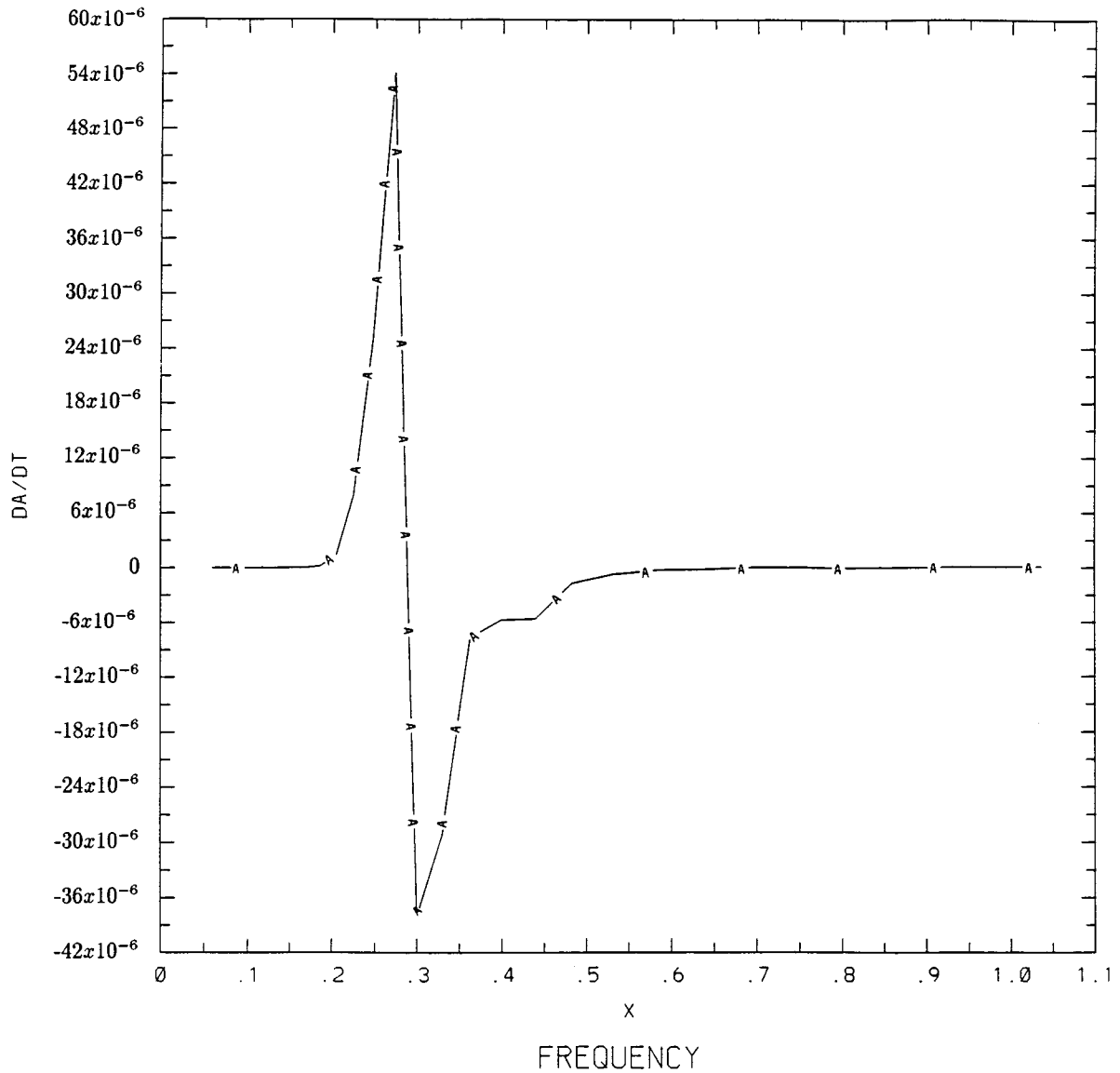


Figure A5. As in Figure A3 with $\Delta f = 0.4f_p$ and $\Delta\theta = 60^\circ$.



(NCWM, DEPTH=1000M, LINEAR DISPERSION)

Figure A6. Total nonlinear transfer from (6), as shown in Figure 3, with lower angular ($D\theta = 30^\circ$) and frequency ($df_i = 0.1f_{i-1}$) resolutions.

$df_i = 0.1f_{i-1}$, the corresponding nonlinear transfer DA/DT from the full integration of (6), as shown in Figure A6, is an order of magnitude smaller than the corresponding results shown in Figure 4a.

Acknowledgments. This research is funded in part by the Wave Prediction Base Enhancement Program of the Office of Naval Research. The wave modeling program at BIO is funded by the Federal Panel on Energy Research and Development (Canada) under Project 534201. The authors would like to express their thanks to Zakharov of the University of Arizona and Shirshov Institute of Oceanology (Moscow) for his valuable discussions. We would also like to thank Dyachenko and Lvov of the University of Arizona for sharing their results with us. We are very grateful to A. Masuda of Kyushu University for discussions and results on the variation of the nonlinear transfer with depth.

References

- Cardone, V. D., R. E. Jensen, D. T. Resio, V. R. Swail, and A. T. Cox, Evolution of contemporary ocean wave models in rare extreme events: "Halloween Storm" of October, 1991; "Storm of the Century" of March, 1993, *J. Atmos. Oceanic Technol.*, **13**, 198–230, 1995.
- Crawford, D. R., B. M. Lake, P. G. Saffman, and H. C. Yuen, Stability of weakly nonlinear deep-water waves in two and three dimensions, *J. Fluid Mech.*, **105**, 177–191, 1981.
- Dyachenko, A. I., and Y. V. Lvov, On the Hasselmann's and Zakharov's approaches to the kinetic equations for the gravity waves, *J. Phys. Oceanogr.*, **25**(12), 3237–3238, 1994.
- Eldeberky, Y., Nonlinear transformation of wave spectra in the near-shore zone, Ph.D. thesis, 203 pp., Delft Univ., 1996.
- Fox, M. J. H., On the nonlinear transfer of energy in the peak of a gravity-wave spectrum II, *Proc. R. Soc. London, Ser. A*, **348**, 467–483, 1976.
- Hashimoto, N., H. Tsuruya, and Y. Nakagawa, Numerical computa-

- tions of the nonlinear energy transfer of gravity-wave spectra in finite water depths, *Coastal Eng. J. Jpn.*, 40, 23–40, 1998.
- Hasselmann, K., On the nonlinear energy transfer in a gravity-wave spectrum, I, General theory, *J. Fluid Mech.*, 12, 481–500, 1962.
- Hasselmann, K., et al., *The Sea Wave Modelling Project (SWAMP): Principal Results and Conclusions*, 256 pp., Plenum, New York, 1985.
- Hasselmann, S., and K. Hasselmann, A symmetrical method of computing the nonlinear transfer in a gravity-wave spectrum, *Hamb. Geophys. Einzelschriften Reihe A Wiss. Abhand.*, 52, 138 pp., 1981.
- Hasselmann, S., and K. Hasselmann, Computation and parameterizations of the nonlinear energy transfer in a gravity-wave spectrum, I, A new method for efficient computations of the exact nonlinear transfer integral, *J. Phys. Oceanogr.*, 15, 1369–1377, 1985.
- Hasselmann, S., K. Hasselmann, J. H. Alleder, and T. P. Barnett, Computations and parameterizations of nonlinear energy transfer in gravity-wave spectrum, II, Parameterizations of the nonlinear energy transfer for application in wave models, *J. Phys. Oceanogr.*, 15, 1378–1391, 1985.
- Hasselmann, S., K. Hasselmann, G. K. Komen, P. Janssen, J. A. Ewing, and V. Cardone, The WAM model—A third generation ocean wave prediction model, *J. Phys. Oceanogr.*, 18, 1775–1810, 1988.
- Herterich, K., and K. Hasselmann, A similarity relation for the nonlinear energy transfer in a finite depth gravity-wave spectrum, *J. Fluid Mech.*, 97, 215–224, 1980.
- Jackson, J. D., *Classical Electrodynamics*, John Wiley, New York, 1962.
- Jensen, R., D. Resio, R.-Q. Lin, G. V. Vledder, T. Herbers, B. Tracy, and L. Vincent, A report of nonlinear source function computational workshop, *ONR Annu. Rep.*, 1998.
- Komen, G. J., L. Cavaleri, M. Donelan, K. Hasselmann, and P. A. E. M. Janssen, *Dynamics and Modelling of Ocean Waves*, 512 pp., Cambridge University Press, New York, 1994.
- Lin, R. Q., and W. Perrie, A new coast wave model, III, Nonlinear wave-wave interaction for wave spectral evolution, *J. Phys. Oceanogr.*, 27, 1813–1826, 1997.
- Longuet-Higgins, M. S., On the theory of the nonlinear transfer of energy in the peak of gravity-wave spectrum: A simplified model, *Proc. R. Soc. London, Ser. A*, 347, 311–328, 1976.
- Masada, A., Nonlinear energy transfer between wind waves, *J. Phys. Oceanogr.*, 15, 1369–1377, 1980.
- Phillips, O. M., On the dynamics of unsteady gravity waves of finite amplitude, *J. Fluid Mech.*, 9, 193–217, 1960.
- Polnikov, V. G., Nonlinear energy transfer through spectrum of gravity waves for the finite depth case, *J. Phys. Oceanogr.*, 27, 1481–1481, 1997.
- Resio, D., and W. Perrie, A numerical study of nonlinear energy fluxes due to wave-wave interactions, I, Methodology and basic results, *J. Fluid Mech.*, 223, 603–629, 1991.
- Snyder, R. L., W. C. Thacker, K. Hasselmann, S. Hasselmann, and G. Barzel, Implementation of an efficient scheme for calculating nonlinear transfer from wave-wave interaction, *J. Geophys. Res.*, 98, 14,507–14,525, 1993.
- Tracy, B. A., and D. T. Resio, Theory and calculation of the nonlinear energy transfer between sea waves in deep water, *WIS Rep. 11*, 50 pp., U.S. Army Eng. Waterways Exp. Station, Vicksburg, Miss., 1982.
- Webb, D. J., Non-linear transfers between sea waves, *Deep Sea Res.*, 25, 279–298, 1978.
- Young, I. R., and G. P. Van Vledder, A review of the central role of nonlinear interactions in wind-wave evolution, *Philos. Trans. R. Soc. London, Ser. A*, 342, 505–524, 1993.
- Zakharov, V. E., Stability of periodic waves and finite amplitude on the surface of deep fluid, *Zhurnal Prikladnoi Mekhaniki Tekhn. Fiz.*, 3, No. 2, 80–94, 1968.
- Zakharov, V. E., Inverse and direct cascade in wind-driven surface wave turbulent and wave-breaking, in *Breaking Waves, IUTAM Symposium*, edited by M. L. Banner and R. H. J. Grimshaw, pp. 69–91, Springer-Verlag, New York, 1991.
- Zakharov, V. E., Weak nonlinear wave-wave interactions in shallow water, *J. Am. Math Soc. Transl.*, 182, 167–197, 1998.
- Zakharov, V. E., and Filonenko, N. N., The energy spectrum for stochastic oscillation of fluid's surface, *Dokl. Akad. Nauk.*, 170, 1292–1295, 1966.

R. Q. Lin, Hydromechanic Directorate, Code 5500, David Taylor Model Basin, NSWC, Carderock Division, 9500 MacArthur Boulevard, West Bethesda, MD 20817-5700. (rlin@wave2.dt.navy.mil)

W. Perrie, Physical and Chemical Science, Department of Fisheries and Oceans, Bedford Institute of Oceanography, Dartmouth, Nova Scotia, Canada B2Y 4A2.

(Received June 13, 1997; revised August 14, 1998; accepted December 17, 1998.)

